

# Grid-less Variational Bayesian Inference of Line Spectral Estimation from Quantized Samples

Jiang Zhu, Qi Zhang and Xiangming Meng

## Abstract

Efficient estimation of line spectral from quantized samples is of vital importance in information theory and signal processing, e.g., channel estimation in energy efficient massive MIMO systems and direction of arrival estimation. The goal of this paper is to recover the line spectral as well as its corresponding parameters such as model order, frequency and amplitudes from heavily quantized samples. To this end, we propose an efficient grid-less Bayesian algorithm named VALSE-EP, which is based on the variational line spectral estimation (VALSE) and expectation propagation (EP). The basic idea of VALSE-EP is to iteratively approximate the challenging quantized model of line spectral estimation as a sequence of simple pseudo unquantized models, so that the VALSE algorithm can be applied. Note that since the noise in the pseudo linear model is heteroscedastic (different components having different variance), a variant of the VALSE is re-derived to obtain the final VALSE-EP. Moreover, to obtain a benchmark performance of the proposed algorithm, the Cramér Rao bound (CRB) is derived. Finally, numerical results show that the performance of VALSE-EP is close to the CRB, demonstrating effectiveness of VALSE-EP for line spectral estimation from quantized samples.

**keywords:** Variational Bayesian inference, expectation propagation, quantization, line spectral estimation, MMSE, gridless

## I. INTRODUCTION

Line spectral estimation (LSE) is a fundamental problem in statistical signal processing due to its widespread application in channel estimation [1] and direction of arrival (DOA) estimation [2]. On the one hand, many classical methods have been proposed, such as periodogram [3], MUSIC [4] and ESPRIT

Jiang Zhu and Qi Zhang are with the Key Laboratory of Ocean Observation-imaging Testbed of Zhejiang Province, Ocean College, Zhejiang University, No.1 Zheda Road, Zhoushan, 316021, China. Xiangming Meng is with Huawei Technologies, Co. Ltd., Shanghai, 201206, China.

[5]. On the other hand, to exploit the frequency sparsity of the line spectral signal, sparse representation and compressed sensing (CS) based methods have been proposed to estimate frequencies for multiple sinusoids.

Depending on the model adopted, CS based methods for LSE can be classified into three categories, namely, on-grid, off-grid and grid-less, which also corresponds to the chronological order in which they have been developed [6]. At first, grid based method where the continuous frequency is discretized into a finite set of grid points is proposed [7]. It is shown that grid based method will incur basis mismatch when the true frequencies do not lie exactly on the grid [8]. Then, off-the-grid compressed sensing methods have been proposed. In [9], a Newtonalized orthogonal matching pursuit (NOMP) method is proposed, where a Newton step and feedback are utilized to refine the frequency estimates. Compared to the incremental step in updating the frequencies in NOMP approach, the iterative reweighted approach (IRA) [10] estimates the frequencies in parallel, which improves the estimation accuracy at the cost of increasing complexity. In [11], superfast LSE methods are proposed based on fast Toeplitz matrix inversion algorithm. In [12, 13], a sparse Bayesian learning method is proposed, where the grid bias and the grid is jointly estimated [12], or the Newton method is applied to refine the frequency estimates [13]. To completely overcome the grid mismatch problem, grid-less based methods have been proposed [14–17]. The atomic norm-based methods involve solving a semidefinite programming (SDP) problem [18], whose computation complexity is prohibitively high for large problem sizes. In [19], a grid-less variational line spectral estimation (VALSE) algorithm is proposed, where posterior probability density function (PDF) of the frequency is provided. In [20], the multisnapshot VALSE (MVALSE) is developed for the MMVs setting, and it shows the relationship between the VALSE and the MVALSE.

In practice, the measurements can be obtained in a nonlinear way. For example, in the mmWave multiple input multiple output (MIMO) system, since the mmWave accompanies large bandwidths, the cost and power consumption are huge due to high precision (e.g., 10-12 bits) analog-to-digital converters (ADCs) [21]. Consequently, low precision ADCs (often 1 – 3 bits) are adopted to alleviate the ADC bottleneck. Another motivation is wideband spectrum sensing in bandwidth-constrained wireless networks [22, 23]. In order to reduce the communication overhead, the sensors quantize their measurements into a single bit, and the spectrum is estimated from the heavily quantized measurements at the fusion center (FC). Thus it is meaningful to design efficient recovery algorithms under low precision quantized observations [24, 25].

### A. Related Work

Many classical methods have been extended to solve the LSE from quantized samples. In [26], the spectrum of the one-bit data is analyzed, which consists of plentiful harmonics. It shows that under low signal to noise ratio (SNR) scenario, the amplitudes of the higher order harmonics is much smaller than that of the fundamental frequency, thus the classical FFT based method still works well for the SAR imaging experiment. However, the FFT based method can overestimate the model order (number of spectrums) for high SNR scenario. As a consequence, the quantization effects must be taken into consideration. The CS based methods have been proposed to solve the LSE from quantized samples, which can also be classified into on-grid, off-grid and grid-less methods.

- on-grid method: The on-grid method can be classified into  $l_1$  minimization based approach [27–29] and generalized sparse Bayesian learning (Gr-SBL) [30] algorithm. For  $l_1$  minimization approach, the regularization parameter is hard to determine the tradeoff between the fitting error and the sparsity. The computation complexity of the Gr-SBL is high, as it involves a matrix inversion in each iteration. While, the reconstruction accuracy of the Gr-SBL is high.
- off-grid method: The SVM based [31] and 1bRelax algorithm [32] are two approaches. For the SVM based approach, the model order needs to be known in advance. While for the 1bRelax algorithm, [33] derives the consistent Bayesian information criterion (BIC) to determine the model order.
- grid-less method: The grid-less approach can completely overcome the grid mismatch. For quantization setting, the atom norm minimization based approach has been proposed [34–36], whose computation complexity is high as it involves solving a SDP.

Form the CS algorithm point of view, many Bayesian algorithms have been developed, such as approximate message passing (AMP) [39], vector AMP (VAMP) [43]. Later, it is shown that both AMP and VAMP can be derived via expectation propagation (EP) [40, 41], which is an effective approximate Bayesian inference method [37]. In [38], a unified Bayesian inference framework has been proposed, which shows that the GLM can be iteratively approximated as a standard linear model (SLM), and many standard Bayesian algorithms can be extended to solve the GLM. For example, AMP [39], VAMP [43], SBL [45] can be easily extended to generalized AMP [42], generalized VAMP (GVAMP) [44], and generalized SBL (Gr-SBL) algorithm [30, 38]. This work extends the idea and utilize EP to solve the LSE from quantized samples.

### B. Main Contributions

This work studies the LSE from quantized measurements. Utilizing the expectation propagation (EP) [37], the generalized linear model can be iteratively decomposed as two modules (a standard linear model

<sup>1</sup> and a componentwise minimum mean square error (MMSE) module) [38]. Thus the VALSE algorithm is run in the standard linear module where the frequency estimate is iteratively refined. For the MMSE module, it refines the pseudo observations of the linear model <sup>2</sup>. By iterating between the two modules, it improves the frequency estimates gradually. The main contributions of this work are summarized as follows:

- A VALSE-EP method is proposed to deal with the LSE from quantized samples. This method is a completely grid-less method and the computation complexity is low, compared to the atom minimization approach.
- The model order estimation and the algorithm is coupled together, which reduces the computation complexity.
- Compared to the existing method which only provides the point estimates of the frequency, VALSE-EP outputs the uncertain degrees of the estimates, i.e., the posterior PDF of the frequency, and thus VALSE-EP can be easily extended to perform sequential estimation from nonlinear measurements.
- Utilizing the framework from [38], VALSE-EP is proposed which combines the VALSE algorithm with EP. The two different criteria combined together, and excellent performance is shown numerically.

### C. Paper Organization and Notation

The rest of this paper is organized as below. Section II describes the signal model and introduces the probabilistic formulation. Section III derives the Cramér bound (CRB). Section IV develops the VALSE-EP algorithm and the details of the updating expressions are presented. Substantial numerical experiments are provided in Section V and Section VI concludes the paper.

For a complex vector  $\mathbf{x} \in \mathbb{C}^M$ , let  $\Re\{\mathbf{x}\}$  and  $\Im\{\mathbf{x}\}$  denote the real and imaginary part of  $\mathbf{x}$ , respectively. Let  $j$  denotes the imaginary number. Let  $\mathcal{S} \subset \{1, \dots, N\}$  be a subset of indices and  $|\mathcal{S}|$  denote its cardinality. For the matrix  $\mathbf{J} \in \mathbb{C}^{N \times N}$ , let  $\mathbf{J}_{\mathcal{S}}$  denote the submatrix by choosing both the rows and columns of  $\mathbf{J}$  indexed by  $\mathcal{S}$ . Similarly, let  $\mathbf{h}_{\mathcal{S}}$  denote the subvector by choosing the elements of  $\mathbf{h}$  indexed by  $\mathcal{S}$ . Let  $(\cdot)_{\mathcal{S}}^*$ ,  $(\cdot)_{\mathcal{S}}^T$  and  $(\cdot)_{\mathcal{S}}^H$  be the conjugate, transpose and Hermitian transpose operator of  $(\cdot)_{\mathcal{S}}$ , respectively. For the matrix  $\mathbf{A}$ , let  $|\mathbf{A}|$  denote the elementwise absolute value of  $\mathbf{A}$ . Let  $\mathbf{I}_L$  denote the identity matrix of dimension  $L$ . “ $\sim i$ ” denotes the indices  $\mathcal{S}$  excluding  $i$ . Let  $\mathcal{CN}(\mathbf{x}; \boldsymbol{\mu}, \boldsymbol{\Sigma})$  denote

<sup>1</sup>In fact, it is a nonlinear model instead of a standard linear model in this paper, as the frequencies are unknown.

<sup>2</sup>Iteratively approximating the generalized linear model as a standard linear model is very beneficial, as many well developed methods such as the information-theoretically optimal successive interference cancellation (SIC) is developed in the SLM.

the complex normal distribution of  $\mathbf{x}$  with mean  $\boldsymbol{\mu}$  and covariance  $\boldsymbol{\Sigma}$ . Let  $\phi(x) = \exp(-x^2/2)/\sqrt{2\pi}$  and  $\Phi(x) = \int_{-\infty}^x \phi(t)dt$  denote the standard normal probability density function (PDF) and cumulative distribution function (CDF), respectively.

## II. PROBLEM SETUP

Let  $\mathbf{z}_N \in \mathbb{C}^N$  be a line spectrum signal consisting of  $K$  complex sinusoids

$$\mathbf{z}_N = \sum_{k=1}^K \mathbf{a}_N(\tilde{\theta}_k) \tilde{w}_k, \quad (1)$$

where  $\tilde{w}_k$  is the complex amplitude of the  $k$ th frequency,  $\tilde{\theta}_k \in [-\pi, \pi)$  is the  $k$ th frequency, and

$$\mathbf{a}_N(\theta) = [1, e^{j\theta}, \dots, e^{j(N-1)\theta}]^T. \quad (2)$$

Suppose that only  $M \leq N$  noisy measurements of those components of  $\mathbf{z}_N$  are observed and are quantized into a finite number of bits, i.e.,

$$\mathbf{y} = \mathcal{Q}(\Re\{\mathbf{z}_M + \mathbf{n}\}) + j\mathcal{Q}(\Im\{\mathbf{z}_M + \mathbf{n}\}), \quad (3)$$

where  $\mathbf{z}_M = \sum_{k=1}^K \mathbf{a}_M(\tilde{\theta}_k) \tilde{w}_k$ ,

$$\mathbf{a}_M(\theta) = [e^{jm_1\theta}, e^{jm_2\theta}, \dots, e^{jm_M\theta}]^T, \quad (4)$$

$\mathcal{M} = \{m_1, \dots, m_M\} \subseteq \{0, 1, \dots, N-1\}$ ,  $\mathbf{n} \sim \mathcal{CN}(\mathbf{n}; \mathbf{0}, \sigma^2 \mathbf{I}_M)$ ,  $\sigma^2$  is the variance of the noise. To simplify the notation, in the following text,  $\mathbf{a}(\theta)$  is used instead of  $\mathbf{a}_M(\theta)$ .

The goal of LSE is to jointly recover the number of spectrums  $\hat{K}$  (also named model order), the set of frequencies  $\hat{\boldsymbol{\theta}} = \{\hat{\theta}_k\}_{k=1}^{\hat{K}}$ , the corresponding coefficients  $\{\hat{w}_k\}_{k=1}^{\hat{K}}$  and the LSE  $\hat{\mathbf{z}}_N = \sum_{k=1}^{\hat{K}} \hat{\mathbf{a}}_N(\hat{\theta}_k) \hat{w}_k$  from quantized measurements  $\mathbf{y}$ .

Since the sparsity level  $K$  is usually unknown, the line spectral signal consisting of  $N$  complex sinusoids is assumed [19]

$$\mathbf{z} = \sum_{i=1}^N w_i \mathbf{a}(\theta_i) \triangleq \mathbf{A}(\boldsymbol{\theta}) \mathbf{w}, \quad (5)$$

where  $\mathbf{A}(\boldsymbol{\theta}) = [\mathbf{a}(\theta_1), \dots, \mathbf{a}(\theta_N)]$  and  $N$  satisfies  $N > K$ . Since the number of frequencies is  $K$ , the binary hidden variables  $\mathbf{s} = [s_1, \dots, s_N]^T$  are introduced, where  $s_i = 1$  means that the  $i$ th frequency is active, otherwise deactive ( $w_i = 0$ ). The probability mass function of  $s_i$  is

$$p(s_i) = \rho^{s_i} (1 - \rho)^{(1-s_i)}, \quad s_i \in \{0, 1\}. \quad (6)$$

Given that  $s_i = 1$ , we assume that  $w_i \sim \mathcal{CN}(w_i; 0, \tau)$ . Thus  $(s_i, w_i)$  follows a Bernoulli-Gaussian distribution, that is

$$p(w_i|s_i; \tau) = (1 - s_i)\delta(w_i) + s_i\mathcal{CN}(w_i; 0, \tau). \quad (7)$$

From (6) and (7), it can be seen that the parameter  $\rho$  denotes the probability of the  $i$ th component being active and  $\tau$  is a variance parameter. The variable  $\boldsymbol{\theta} = [\theta_1, \dots, \theta_N]^T$  has the prior PDF  $p(\boldsymbol{\theta}) = \prod_{i=1}^N p(\theta_i)$ . Without any knowledge of the frequency  $\theta$ , the uninformative prior distribution  $p(\theta_i) = 1/(2\pi)$  is used [19]. For encoding the prior distribution, please refer to [19, 20] for further details.

Given  $\mathbf{z}$ , the PDF  $p(\mathbf{y}|\mathbf{z})$  of  $\mathbf{y}$  can be easily calculated through (3). Let

$$\boldsymbol{\Omega} = (\theta_1, \dots, \theta_N, (\mathbf{w}, \mathbf{s})), \quad (8)$$

$$\boldsymbol{\beta} = \{\rho, \tau\} \quad (9)$$

be the set of all random variables and the model parameters, respectively. According to the Bayes rule, the joint PDF  $p(\mathbf{y}, \mathbf{z}, \boldsymbol{\Omega}; \boldsymbol{\beta})$  is

$$p(\mathbf{y}, \mathbf{z}, \boldsymbol{\Omega}; \boldsymbol{\beta}) = p(\mathbf{y}|\mathbf{z})\delta(\mathbf{z} - \mathbf{A}(\boldsymbol{\theta})\mathbf{w}) \prod_{i=1}^N p(\theta_i)p(w_i|s_i)p(s_i). \quad (10)$$

Given the above joint PDF (10), the type II maximum likelihood (ML) estimation of the model parameters  $\hat{\boldsymbol{\beta}}_{\text{ML}}$  is

$$\hat{\boldsymbol{\beta}}_{\text{ML}} = \underset{\boldsymbol{\beta}}{\operatorname{argmax}} p(\mathbf{y}; \boldsymbol{\beta}) = \int p(\mathbf{y}, \mathbf{z}, \boldsymbol{\Omega}; \boldsymbol{\beta}) d\mathbf{z} d\boldsymbol{\Omega}. \quad (11)$$

Then the minimum mean square error (MMSE) estimate of the parameters  $(\mathbf{z}, \boldsymbol{\Omega})$  is

$$(\hat{\mathbf{z}}, \hat{\boldsymbol{\Omega}}) = \mathbb{E}[(\mathbf{z}, \boldsymbol{\Omega})|\tilde{\mathbf{y}}; \boldsymbol{\beta}_{\text{ML}}], \quad (12)$$

where the expectation is taken with respect to

$$p(\mathbf{z}, \boldsymbol{\Omega}|\mathbf{y}; \hat{\boldsymbol{\beta}}_{\text{ML}}) = \frac{p(\mathbf{z}, \boldsymbol{\Omega}, \mathbf{y}; \hat{\boldsymbol{\beta}}_{\text{ML}})}{p(\mathbf{y}; \hat{\boldsymbol{\beta}}_{\text{ML}})} \quad (13)$$

Directly solving the ML estimate of  $\boldsymbol{\beta}$  (11) or the MMSE estimate of  $(\mathbf{z}, \boldsymbol{\Omega})$  (12) are both intractable. As a result, an iterative algorithm is designed in Section IV.

### III. CRAMÉR RAO BOUND

Before designing the recovery algorithm, the performance bounds of unbiased estimators are derived, i.e., the Cramér Rao bound (CRB). Although the Bayesian algorithm is designed, the CRB can be acted as the performance benchmark of the algorithm. To derive the CRB,  $K$  is assumed to be known, the frequencies  $\boldsymbol{\theta} \in \mathbb{R}^K$  and weights  $\mathbf{w} \in C^K$  are treated as deterministic unknown parameters. As

for the quantizer  $Q(\cdot)$ , the quantization intervals are  $\{(t_l, t_{l+1})\}_{l=0}^{|\mathcal{D}|-1}$ , where  $t_0 = -\infty$ ,  $t_{\mathcal{D}} = \infty$ ,  $\bigcup_{l=0}^{|\mathcal{D}|-1} [t_l, t_{l+1}) = \mathbb{R}$ . Given a real number  $a \in [t_l, t_{l+1})$ , the representation is

$$Q(a) = \omega_l, \quad \text{if } a \in [t_l, t_{l+1}). \quad (14)$$

Note that for a quantizer with bit-depth  $B$ , the cardinality of the output of the quantizer is  $|\mathcal{D}| = 2^B$ . Let  $\boldsymbol{\kappa}$  denote the set of parameters, i.e.,  $\boldsymbol{\kappa} = [\boldsymbol{\theta}^T, \Re\{\mathbf{w}^T\}, \Im\{\mathbf{w}^T\}]^T \in \mathbb{R}^{3K}$ . The probability mass function (PMF) of the measurements  $p(\mathbf{y}|\boldsymbol{\kappa})$  is

$$p(\mathbf{y}|\boldsymbol{\kappa}) = \prod_{i=1}^M p(y_i|\boldsymbol{\kappa}) = \prod_{i=1}^M p(\Re\{y_i\}|\boldsymbol{\kappa})p(\Im\{y_i\}|\boldsymbol{\kappa}). \quad (15)$$

Moreover, the PMFs of  $\Re\{y_i\}$  and  $\Im\{y_i\}$  are

$$p(\Re\{y_i\}|\boldsymbol{\kappa}) = \prod_{\omega_l \in \mathcal{D}} p_{\Re\{y_i\}}(\omega_l|\boldsymbol{\kappa}) I_{Q(\Re\{y_i\})=\omega_l}, \quad (16)$$

$$p(\Im\{y_i\}|\boldsymbol{\kappa}) = \prod_{\omega_l \in \mathcal{D}} p_{\Im\{y_i\}}(\omega_l|\boldsymbol{\kappa}) I_{Q(\Im\{y_i\})=\omega_l}, \quad (17)$$

where  $I_{(\cdot)}$  is the indicator function,

$$\begin{aligned} p_{\Re\{y_i\}}(\omega_l|\boldsymbol{\kappa}) &= \mathbb{P}(\Re\{y_i\} \in [t_l, t_{l+1})) \\ &= \Phi\left(\frac{t_{l+1} - \Re\{z_i\}}{\sigma/\sqrt{2}}\right) - \Phi\left(\frac{t_l - \Re\{z_i\}}{\sigma/\sqrt{2}}\right), \end{aligned} \quad (18)$$

$$\begin{aligned} p_{\Im\{y_i\}}(\omega_l|\boldsymbol{\kappa}) &= \mathbb{P}(\Im\{y_i\} \in [t_l, t_{l+1})) \\ &= \Phi\left(\frac{t_{l+1} - \Im\{z_i\}}{\sigma/\sqrt{2}}\right) - \Phi\left(\frac{t_l - \Im\{z_i\}}{\sigma/\sqrt{2}}\right). \end{aligned} \quad (19)$$

The CRB is equal to the inverse of the Fisher information matrix (FIM)  $\mathbf{I}(\boldsymbol{\kappa}) \in \mathbb{R}^{3K \times 3K}$

$$\mathbf{I}(\boldsymbol{\kappa}) = \mathbb{E} \left[ \left( \frac{\partial \log p(\mathbf{y}|\boldsymbol{\kappa})}{\partial \boldsymbol{\kappa}} \right) \left( \frac{\partial \log p(\mathbf{y}|\boldsymbol{\kappa})}{\partial \boldsymbol{\kappa}} \right)^T \right]. \quad (20)$$

To calculate the FIM, the following Theorem [35] is utilized.

**Theorem 1** [35] *The FIM  $\mathbf{I}(\boldsymbol{\kappa})$  for estimating the unknown parameter  $\boldsymbol{\kappa}$  is*

$$\mathbf{I}(\boldsymbol{\kappa}) = \sum_{i=1}^M \left( \lambda_i \frac{\partial \Re\{z_i\}}{\partial \boldsymbol{\kappa}} \left( \frac{\partial \Re\{z_i\}}{\partial \boldsymbol{\kappa}} \right)^T + \chi_i \frac{\partial \Im\{z_i\}}{\partial \boldsymbol{\kappa}} \left( \frac{\partial \Im\{z_i\}}{\partial \boldsymbol{\kappa}} \right)^T \right). \quad (21)$$

For a general quantizer, one has

$$\lambda_i = \frac{2}{\sigma^2} \sum_{l=0}^{|\mathcal{D}|-1} \frac{[\phi(\frac{t_{l+1} - \Re\{z_i\}}{\sigma/\sqrt{2}}) - \phi(\frac{t_l - \Re\{z_i\}}{\sigma/\sqrt{2}})]^2}{\Phi(\frac{t_{l+1} - \Re\{z_i\}}{\sigma/\sqrt{2}}) - \Phi(\frac{t_l - \Re\{z_i\}}{\sigma/\sqrt{2}})}, \quad (22)$$

and

$$\chi_i = \frac{2}{\sigma^2} \sum_{l=0}^{|\mathcal{D}|-1} \frac{[\phi(\frac{t_{l+1}-\Im\{z_i\}}{\sigma/\sqrt{2}}) - \phi(\frac{t_l-\Im\{z_i\}}{\sigma/\sqrt{2}})]^2}{\Phi(\frac{t_{l+1}-\Im\{z_i\}}{\sigma/\sqrt{2}}) - \Phi(\frac{t_l-\Im\{z_i\}}{\sigma/\sqrt{2}})}, \quad (23)$$

For the unquantized system, the FIM is

$$\begin{aligned} \mathbf{I}_{\text{unq}}(\boldsymbol{\kappa}) &= \frac{2}{\sigma^2} \sum_{i=1}^M \left( \frac{\partial \Re\{z_i\}}{\partial \boldsymbol{\kappa}} \left( \frac{\partial \Re\{z_i\}}{\partial \boldsymbol{\kappa}} \right)^\top \right. \\ &\quad \left. + \frac{\partial \Im\{z_i\}}{\partial \boldsymbol{\kappa}} \left( \frac{\partial \Im\{z_i\}}{\partial \boldsymbol{\kappa}} \right)^\top \right). \end{aligned} \quad (24)$$

According to Theorem 1, we need to calculate  $\frac{\partial \Re\{z_i\}}{\partial \boldsymbol{\kappa}}$  and  $\frac{\partial \Im\{z_i\}}{\partial \boldsymbol{\kappa}}$ . In our setting, we have

$$\Re\{\mathbf{z}\} = \Re\{\mathbf{A}\}\Re\{\mathbf{w}\} - \Im\{\mathbf{A}\}\Im\{\mathbf{w}\}, \quad (25)$$

$$\Im\{\mathbf{z}\} = \Re\{\mathbf{A}\}\Im\{\mathbf{w}\} + \Im\{\mathbf{A}\}\Re\{\mathbf{w}\}. \quad (26)$$

We need to calculate  $\frac{\partial \Re\{z_i\}}{\partial \boldsymbol{\kappa}}$  and  $\frac{\partial \Im\{z_i\}}{\partial \boldsymbol{\kappa}}$ . We have, for  $k = 1, \dots, K$ ,

$$\begin{aligned} \frac{\partial \Re\{z_i\}}{\partial \theta_k} &= -m_i (\sin(m_i \theta_k) \Re\{w_k\} + \cos(m_i \theta_k) \Im\{w_k\}), \\ \frac{\partial \Re\{z_i\}}{\partial \Re\{w_k\}} &= \Re\{A_{ik}\} = \cos(m_i \theta_k), \\ \frac{\partial \Re\{z_i\}}{\partial \Im\{w_k\}} &= -\Im\{A_{ik}\} = -\sin(m_i \theta_k), \\ \frac{\partial \Im\{z_i\}}{\partial \theta_k} &= -m_i (\sin(m_i \theta_k) \Im\{w_k\} - \cos(m_i \theta_k) \Re\{w_k\}), \\ \frac{\partial \Im\{z_i\}}{\partial \Re\{w_k\}} &= \Re\{A_{ik}\} = \cos(m_i \theta_k), \\ \frac{\partial \Im\{z_i\}}{\partial \Im\{w_k\}} &= \Im\{A_{ik}\} = \sin(m_i \theta_k). \end{aligned}$$

The CRB for the quantized and unquantized settings are  $\text{CRB}(\boldsymbol{\kappa}) = \mathbf{I}^{-1}(\boldsymbol{\kappa})$  and  $\text{CRB}_{\text{unq}}(\boldsymbol{\kappa}) = \mathbf{I}_{\text{unq}}^{-1}(\boldsymbol{\kappa})$ , respectively. The CRB of the frequencies are  $[\text{CRB}(\boldsymbol{\kappa})]_{1:K, 1:K}$ , which will be used as the performance metrics.

#### IV. VALSE-EP ALGORITHM

In this section, the EP-VALSE algorithm is developed based on EP. For a given target distribution  $p$ , by restricting the approximate distribution  $q$  into an exponential family (often Gaussian) set  $\Phi$ , EP aims to minimize the Kullback-Leibler divergence  $\text{KL}(p||q)$ , i.e.,  $q = \underset{q \in \Phi}{\text{argmin}} \text{KL}(p||q)$ . For Gaussian distribution set  $\Phi$ , EP amounts to moment matching, i.e., the first and second moment of  $p$  equals to that of  $q$ . According to EP and the factor graph presented in Fig. 1, the quantization model is iteratively

reduced to a sequence of pseudo unquantized model. As a result, the original quantized LSE problem is decoupled into two modules: the componentwise MMSE module and the VALSE module. The two modules iteratively exchange the extrinsic information and refine their estimates. The detailed VALSE-EP is presented as follows.

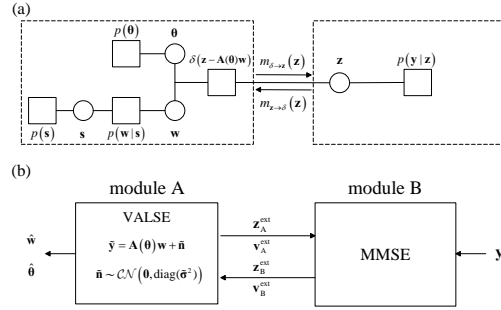


Fig. 1. Factor graph of the joint PDF (10) and the module of the VALSE-EP algorithm. Here the circle denotes the variable node, and the square denotes the factor node. According to the dashed block diagram in Fig. 1 (a), the problem can be decomposed as two modules in Fig. 1 (b), where module A corresponds to the standard linear model, and module B corresponds to the MMSE estimation. Intuitively, the problem can be solved by iterating between the two modules, where module A performs the standard VALSE algorithm, and module B performs the componentwise MMSE estimation.

### A. Componentwise MMSE module

The factor graph and the algorithm module as shown in Fig. 1. Specifically, in the  $t$ th iteration, let  $m_{\delta \rightarrow \mathbf{z}}^t(\mathbf{z}) = \mathcal{CN}(\mathbf{z}_A^{\text{ext}}(t), \text{diag}(\mathbf{v}_A^{\text{ext}}(t)))$  denote the message transmitted from the factor node  $\delta(\mathbf{z} - \mathbf{A}\mathbf{w})$  to the variable node  $\mathbf{z}$ . According to EP, the message  $m_{\mathbf{z} \rightarrow \delta}^t(\mathbf{z})$  transmitted from the variable node  $\mathbf{z}$  to the factor node  $\delta(\mathbf{z} - \mathbf{A}\mathbf{w})$  can be calculated as [37]

$$m_{\mathbf{z} \rightarrow \delta}^t(\mathbf{z}) \propto \frac{\text{Proj}[m_{\delta \rightarrow \mathbf{z}}^t(\mathbf{z})p(\mathbf{y}|\mathbf{z})]}{m_{\delta \rightarrow \mathbf{z}}^t(\mathbf{z})} \triangleq \frac{\text{Proj}[q_B^t(\mathbf{z})]}{m_{\delta \rightarrow \mathbf{z}}^t(\mathbf{z})}, \quad (27)$$

where  $\propto$  denotes identity up to a normalizing constant. First, the MMSE estimate of  $\mathbf{z}$  can be obtained, i.e.,

$$\mathbf{z}_B^{\text{post}}(t) = \mathbb{E}[\mathbf{z}|q_B^t(\mathbf{z})], \quad (28)$$

$$\mathbf{v}_B^{\text{post}}(t) = \text{Var}[\mathbf{z}|q_B^t(\mathbf{z})], \quad (29)$$

where  $E[\cdot|q_B^t(\mathbf{z})]$  and  $\text{Var}[\cdot|q_B^t(\mathbf{z})]$  are the mean and variance operations taken componentwise with respect to the distribution  $\propto q_B^t(\mathbf{z})$ . As a result,  $\text{Proj}[q_B^t(\mathbf{z})]$  is <sup>3</sup>

$$\text{Proj}[q_B^t(\mathbf{z})] = \mathcal{CN}(\mathbf{z}; \mathbf{z}_B^{\text{post}}(t), \text{diag}(\mathbf{v}_B^{\text{post}}(t))). \quad (30)$$

Substituting (30) in (27), the message  $m_{\mathbf{z} \rightarrow \delta}^t(\mathbf{z})$  from the variable node  $\mathbf{z}$  to the factor node  $\delta(\mathbf{z} - \mathbf{A}\mathbf{x})$  is calculated as

$$m_{\mathbf{z} \rightarrow \delta}^t(\mathbf{z}) \propto \frac{\mathcal{CN}(\mathbf{z}; \mathbf{z}_B^{\text{post}}(t), \text{diag}(\mathbf{v}_B^{\text{post}}(t)))}{\mathcal{CN}(\mathbf{z}; \mathbf{z}_A^{\text{ext}}(t), \text{diag}(\mathbf{v}_A^{\text{ext}}(t)))} \propto \mathcal{CN}(\mathbf{z}; \mathbf{z}_B^{\text{ext}}(t), \text{diag}(\mathbf{v}_B^{\text{ext}}(t))), \quad (31)$$

where  $\mathbf{z}_B^{\text{ext}}(t)$  and  $\mathbf{v}_B^{\text{ext}}(t)$  are [38]

$$\mathbf{v}_B^{\text{ext}}(t) = \left( \frac{1}{\mathbf{v}_B^{\text{post}}(t)} - \frac{1}{\mathbf{v}_A^{\text{ext}}(t)} \right)^{-1}, \quad (32a)$$

$$\mathbf{z}_B^{\text{ext}}(t) = \mathbf{v}_B^{\text{ext}}(t) \odot \left( \frac{\mathbf{z}_B^{\text{post}}(t)}{\mathbf{v}_B^{\text{post}}(t)} - \frac{\mathbf{z}_A^{\text{ext}}(t)}{\mathbf{v}_A^{\text{ext}}(t)} \right), \quad (32b)$$

where  $\odot$  denotes componentwise multiplication.

### B. VALSE module

According to (31), the message  $m_{\mathbf{z} \rightarrow \delta}^t(\mathbf{z})$  transmitted from the variable node  $\mathbf{z}$  to the factor node  $\delta(\mathbf{z} - \mathbf{A}\mathbf{x})$  is Gaussian distributed. Based on the definition of the factor node  $\delta(\mathbf{z} - \mathbf{A}\mathbf{x})$ , a pseudo linear observation model

$$\tilde{\mathbf{y}}(t) = \mathbf{A}(\boldsymbol{\theta})\mathbf{w} + \tilde{\mathbf{n}}(t), \quad (33)$$

is obtained, where  $\tilde{\mathbf{n}}(t) \sim \mathcal{CN}(\mathbf{0}, \text{diag}(\tilde{\boldsymbol{\sigma}}^2(t)))$ ,  $\tilde{\mathbf{y}}(t) = \mathbf{z}_B^{\text{ext}}(t)$  and  $\tilde{\boldsymbol{\sigma}}^2(t) = \mathbf{v}_B^{\text{ext}}(t)$ . In [19], the VALSE is derived where the additive Gaussian noise is homogenous while here the additive Gaussian noise is heteroscedastic (independent components having different variance). As a result, modifications are needed to ensure that the original VALSE works. For simplicity, we omit the iteration index  $t$ .

For model (33), the factor graph is also presented in Fig. 2. Given the pseudo observations  $\tilde{\mathbf{y}}$  and nuisance parameters  $\boldsymbol{\beta}$ , the above joint PDF is

$$p(\tilde{\mathbf{y}}, \boldsymbol{\Omega}; \boldsymbol{\beta}) \propto \left( \prod_{i=1}^N p(\theta_i) p(s_i) p(w_i | s_i) \right) p(\tilde{\mathbf{y}} | \boldsymbol{\theta}, \mathbf{w}), \quad (34)$$

where we have used  $p(w_i | s_i)$  and  $p(\tilde{\mathbf{y}} | \boldsymbol{\theta}, \mathbf{w})$  instead of  $p(\mathbf{w}_i | s_i; \tau)$  and  $p(\tilde{\mathbf{y}} | \boldsymbol{\theta}, \mathbf{w}; \boldsymbol{\Sigma}) = \mathcal{CN}(\tilde{\mathbf{y}}; \mathbf{A}(\boldsymbol{\theta})\mathbf{w}, \boldsymbol{\Sigma})$ , and  $\boldsymbol{\Sigma} = \text{diag}(\tilde{\boldsymbol{\sigma}}^2(t))$ . Performing the type II maximum likelihood (ML) estimation of the model parameters  $\hat{\boldsymbol{\beta}}_{\text{ML}}$  are still intractable. Thus variational approach where a given structured PDF  $q(\boldsymbol{\Omega} | \tilde{\mathbf{y}})$  is used

<sup>3</sup>Here the diagonal EP is used. It is numerically shown that the scalar EP which averages the noise variance yields significant performance degradation.

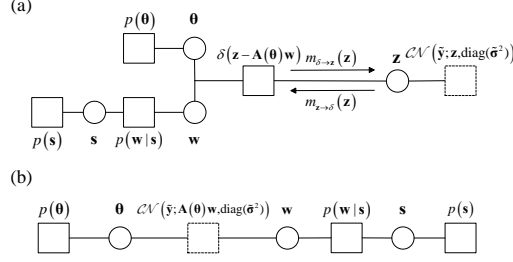


Fig. 2. Two equivalent factor graphs of the joint PDF (34). The dashed square denotes the pseudo factor graph. Also, the factor graph of Fig. 2 (b) is borrowed from [19].

to approximate  $p(\Omega|\tilde{y})$  is adopted, where  $p(\Omega|\tilde{y}) = p(\tilde{y}, \Omega; \beta)/p(\tilde{y}; \beta)$  and  $p(\tilde{y}; \beta) = \int p(\tilde{y}, \Omega; \beta) d\Omega$ . The variational Bayesian uses the Kullback-Leibler (KL) divergence of  $p(\Omega|\tilde{y})$  from  $q(\Omega|\tilde{y})$  to describe their dissimilarity, which is defined as [47, p. 732]

$$\text{KL}(q(\Omega|\tilde{y})||p(\Omega|\tilde{y})) = \int q(\Omega|\tilde{y}) \log \frac{q(\Omega|\tilde{y})}{p(\Omega|\tilde{y})} d\Omega. \quad (35)$$

In general, the posterior PDF  $q(\Omega|\tilde{y})$  is chosen from a distribution set to minimize the KL divergence. The log model evidence  $\ln p(\tilde{y}; \beta)$  for any assumed PDF  $q(\Omega|\tilde{y})$  is [47, pp. 732-733]

$$\ln p(\tilde{y}; \beta) = \text{KL}(q(\Omega|\tilde{y})||p(\Omega|\tilde{y})) + \mathcal{L}(q(\Omega|\tilde{y})), \quad (36)$$

where

$$\mathcal{L}(q(\Omega|\tilde{y})) = \mathbb{E}_{q(\Omega|\tilde{y})} \left[ \ln \frac{p(\tilde{y}; \Omega; \beta)}{q(\Omega|\tilde{y})} \right]. \quad (37)$$

For a given data  $\tilde{y}$ ,  $\ln p(\tilde{y}; \beta)$  is constant, thus minimizing the KL divergence is equivalent to maximizing  $\mathcal{L}(q(\Omega|\tilde{y}))$  in (36). Therefore we maximize  $\mathcal{L}(q(\Omega|\tilde{y}))$  in the sequel.

For the factored PDF  $q(\Omega|\tilde{y})$ , the following assumptions are made:

- Given  $\tilde{y}$ , the frequencies  $\{\theta_i\}_{i=1}^N$  are mutually independent.
- The posterior of the binary hidden variables  $q(s|\tilde{y})$  has all its mass at  $\hat{s}$ , i.e.,  $q(s|\tilde{y}) = \delta(s - \hat{s})$ .
- Given  $\tilde{y}$  and  $s$ , the frequencies and weights are independent.

As a result,  $q(\Omega|\tilde{y})$  can be factored as

$$q(\Omega|\tilde{y}) = \prod_{i=1}^N q(\theta_i|\tilde{y}) q(w|\tilde{y}, s) \delta(s - \hat{s}). \quad (38)$$

Due to the factorization property of (38), the frequency  $\theta$  can be estimated from  $q(\Omega|\tilde{y})$  as [19]

$$\hat{\theta}_i = \arg(\mathbb{E}_{q(\theta_i|\tilde{y})}[e^{j\theta_i}]), \quad (39a)$$

$$\hat{\mathbf{a}}_i = \mathbb{E}_{q(\theta_i|\tilde{y})}[\mathbf{a}_N(\theta_i)], \quad i \in \{1, \dots, N\}, \quad (39b)$$

where  $\arg(\cdot)$  returns the angle. For the given posterior PDF  $q(\mathbf{w}|\mathbf{y}, \hat{\mathbf{s}})$ , the mean and covariance estimates of the weights are calculated as

$$\hat{\mathbf{w}} = E_{q(\mathbf{w}|\tilde{\mathbf{y}})}[w], \quad (40a)$$

$$\hat{C}_{i,j} = E_{q(\mathbf{w}|\tilde{\mathbf{y}})}[w_i w_j^*] - \hat{w}_i \hat{w}_j^*, \quad i, j \in \{1, \dots, N\}. \quad (40b)$$

Given that  $q(\mathbf{s}|\tilde{\mathbf{y}}) = \delta(\mathbf{s} - \hat{\mathbf{s}})$ , the posterior PDF of  $\mathbf{w}$  is

$$q(\mathbf{w}|\tilde{\mathbf{y}}) = \int q(\mathbf{w}|\tilde{\mathbf{y}}, \mathbf{s}) \delta(\mathbf{s} - \hat{\mathbf{s}}) d\mathbf{s} = q(\mathbf{w}|\tilde{\mathbf{y}}, \hat{\mathbf{s}}). \quad (41)$$

Let  $\mathcal{S}$  be the set of indices of the non-zero components of  $\mathbf{s}$ , i.e.,

$$\mathcal{S} = \{i | 1 \leq i \leq N, s_i = 1\}.$$

Analogously, we define  $\hat{\mathcal{S}}$  based on  $\hat{\mathbf{s}}$ . The model order is the cardinality of  $\hat{\mathcal{S}}$ , i.e.,

$$\hat{K} = |\hat{\mathcal{S}}|.$$

Finally, the line spectral  $\mathbf{z} = \sum_{k=1}^K \mathbf{a}(\tilde{\theta}_k) \tilde{w}_k$  is reconstructed as

$$\hat{\mathbf{z}} = \sum_{i \in \hat{\mathcal{S}}} \hat{\mathbf{a}}_i \hat{w}_i.$$

The following procedure is similar to [20]. Maximizing  $\mathcal{L}(q(\mathbf{\Omega}|\tilde{\mathbf{y}}))$  with respect to all the factors is also intractable. Similar to the Gauss-Seidel method [48],  $\mathcal{L}$  is optimized over each factor  $q(\theta_i|\tilde{\mathbf{y}})$ ,  $i = 1, \dots, N$  and  $q(\mathbf{w}, \mathbf{s}|\tilde{\mathbf{y}})$  separately with the others being fixed. Maximizing  $\mathcal{L}(q(\mathbf{\Omega}|\tilde{\mathbf{y}}); \boldsymbol{\beta})$  (37) with respect to the posterior approximation  $q(\mathbf{\Omega}_d|\tilde{\mathbf{y}})$  of each latent variable  $\mathbf{\Omega}_d$ ,  $d = 1, \dots, N + 1$  yields [47, pp. 735, eq. (21.25)]

$$\ln q(\mathbf{\Omega}_d|\tilde{\mathbf{y}}) = E_{q(\mathbf{\Omega} \setminus \mathbf{\Omega}_d|\tilde{\mathbf{y}})}[\ln p(\tilde{\mathbf{y}}, \mathbf{\Omega})] + \text{const}, \quad (42)$$

where the expectation is taken with respect to all the variables  $\mathbf{\Omega}$  except  $\mathbf{\Omega}_d$  and the constant ensures normalization of the PDF. In the following, we detail the procedures.

1) *Inferring the frequencies:* For each  $i = 1, \dots, N$ , we maximize  $\mathcal{L}$  with respect to the factor  $q(\theta_i|\tilde{\mathbf{y}})$ . For  $i \notin \mathcal{S}$ , we have  $q(\theta_i|\tilde{\mathbf{y}}) = p(\theta_i)$ . For  $i \in \mathcal{S}$ , the optimal factor  $q(\theta_i|\tilde{\mathbf{y}})$  can be calculated as [47, pp. 736-737]

$$\ln q(\theta_i|\tilde{\mathbf{y}}) = E_{q(\mathbf{\Omega} \setminus \theta_i|\tilde{\mathbf{y}})}[\ln p(\tilde{\mathbf{y}}, \mathbf{\Omega}; \boldsymbol{\beta})] + \text{const}, \quad (43)$$

Substituting (39) and (40) in (43), one obtains

$$\begin{aligned}
& \ln q(\theta_i|\tilde{\mathbf{y}}) = \mathbb{E}_{q(\boldsymbol{\Omega}|\theta_i|\tilde{\mathbf{y}})}[\ln p(\tilde{\mathbf{y}}, \boldsymbol{\Omega}; \boldsymbol{\beta})] + \text{const} \\
& = \mathbb{E}_{q(\mathbf{z}|\theta_i|\tilde{\mathbf{y}})}[\ln(p(\boldsymbol{\theta})p(\mathbf{s})p(\mathbf{w}|\mathbf{s})p(\tilde{\mathbf{y}}|\boldsymbol{\theta}, \mathbf{w}))] + \text{const} \\
& = \ln p(\theta_i) - \mathbb{E}_{q(\mathbf{z}|\theta_i|\tilde{\mathbf{y}})}[(\tilde{\mathbf{y}} - \mathbf{A}_{\hat{\mathcal{S}}}\mathbf{w}_{\hat{\mathcal{S}}})^H \boldsymbol{\Sigma}^{-1}(\tilde{\mathbf{y}} - \mathbf{A}_{\hat{\mathcal{S}}}\mathbf{w}_{\hat{\mathcal{S}}})] + \text{const} \\
& = \ln p(\theta_i) + \Re\{\boldsymbol{\eta}_i^H \mathbf{a}(\theta_i)\} + \text{const}, \tag{44}
\end{aligned}$$

where the complex vector  $\boldsymbol{\eta}_i$  is given by

$$\boldsymbol{\eta}_i = 2\boldsymbol{\Sigma}^{-1} \left[ \left( \tilde{\mathbf{y}} - \sum_{l \in \hat{\mathcal{S}} \setminus \{i\}} \hat{\mathbf{a}}_l \hat{w}_l \right) \hat{w}_i^* - \sum_{l \in \hat{\mathcal{S}} \setminus \{i\}} \hat{\mathbf{a}}_l \hat{C}_{l,i} \right], \tag{45}$$

where “ $\sim i$ ” denote the indices  $\hat{\mathcal{S}}$  excluding  $i$ ,  $\mathbf{w}_{\hat{\mathcal{S}}}$  denotes the subvector of  $\mathbf{w}$  by choosing the  $\hat{\mathcal{S}}$  rows of  $\mathbf{w}$ . The result is consistent with [19, eq. (17)] when  $\boldsymbol{\Sigma} = \nu \mathbf{I}$ .  $q(\theta_i|\tilde{\mathbf{y}})$  is calculated to be

$$q(\theta_i|\tilde{\mathbf{y}}) \propto p(\theta_i) \exp(\Re\{\boldsymbol{\eta}_i^H \mathbf{a}(\theta_i)\}). \tag{46}$$

Since it is hard to obtain the analytical results (39b) for the PDF (46),  $q(\theta_i|\tilde{\mathbf{y}})$  is approximated as a von Mises approximation. For further details, please refer to [19, Algorithm 2: Heuristic 2].

2) *Inferring the weights and support*: Next we keep  $q(\theta_i|\tilde{\mathbf{y}})$ ,  $i = 1, \dots, N$  fixed and maximize  $\mathcal{L}$  w.r.t.  $q(\mathbf{w}, \mathbf{s}|\tilde{\mathbf{y}})$ . Define the matrices  $\mathbf{J}$  and  $\mathbf{h}$  as

$$J_{ij} = \begin{cases} \text{tr}(\boldsymbol{\Sigma}^{-1}), & i = j \\ \hat{\mathbf{a}}_i^H \boldsymbol{\Sigma}^{-1} \hat{\mathbf{a}}_j, & i \neq j \end{cases}, \quad i, j \in \{1, 2, \dots, N\}, \tag{47a}$$

$$\mathbf{h} = \hat{\mathbf{A}}^H \boldsymbol{\Sigma}^{-1} \tilde{\mathbf{y}}. \tag{47b}$$

According to (42),  $q(\mathbf{w}, \mathbf{s}|\tilde{\mathbf{y}})$  can be calculated as

$$\begin{aligned}
& \ln q(\mathbf{w}, \mathbf{s}|\tilde{\mathbf{y}}) = \mathbb{E}_{q(\boldsymbol{\Omega}|\mathbf{w}, \mathbf{s}|\tilde{\mathbf{y}})}[\ln p(\tilde{\mathbf{y}}, \boldsymbol{\Omega}; \boldsymbol{\beta})] + \text{const} \\
& = \mathbb{E}_{q(\boldsymbol{\theta}|\tilde{\mathbf{y}})} \left[ \sum_{i=1}^N \ln p(s_i) + \ln p(\mathbf{w}|\mathbf{s}) + \ln p(\tilde{\mathbf{y}}|\boldsymbol{\theta}, \mathbf{w}) \right] + \text{const} \\
& = (\mathbf{w}_{\mathcal{S}} - \hat{\mathbf{w}}_{\mathcal{S}})^H \hat{\mathbf{C}}_{\mathcal{S}}^{-1} (\mathbf{w}_{\mathcal{S}} - \hat{\mathbf{w}}_{\mathcal{S}}) + \text{const}, \tag{48}
\end{aligned}$$

where

$$\hat{\mathbf{C}}_{\mathcal{S}} = \left( \mathbf{J}_{\mathcal{S}} + \frac{\mathbf{I}_{|\mathcal{S}|}}{\tau} \right)^{-1}, \tag{49a}$$

$$\hat{\mathbf{w}}_{\mathcal{S}} = \hat{\mathbf{C}}_{\mathcal{S}} \mathbf{h}_{\mathcal{S}}. \tag{49b}$$

It is worth noting that calculating  $\widehat{\mathbf{C}}_{\mathcal{S}}$  and  $\widehat{\mathbf{w}}_{\mathcal{S}}$  involves a matrix inversion. In the Appendix VII-A, it is shown that  $\widehat{\mathbf{C}}_{\mathcal{S}}$  and  $\widehat{\mathbf{w}}_{\mathcal{S}}$  can be updated efficiently.

From (38), the posterior approximation  $q(\mathbf{w}, \mathbf{s}|\tilde{\mathbf{y}})$  can be factored as the product of  $q(\mathbf{w}|\tilde{\mathbf{y}}, \mathbf{s})$  and  $\delta(\mathbf{s} - \widehat{\mathbf{s}})$ . According to the formulation of (48), for a given  $\widehat{\mathbf{s}}$ ,  $q(\mathbf{w}_{\widehat{\mathcal{S}}}|\tilde{\mathbf{y}})$  is a complex Gaussian distribution, and  $q(\mathbf{w}_{\tilde{\mathcal{Y}}}; \widehat{\mathbf{s}})$  is

$$q(\mathbf{w}|\tilde{\mathbf{y}}; \widehat{\mathbf{s}}) = \mathcal{CN}(\mathbf{w}_{\widehat{\mathcal{S}}}; \widehat{\mathbf{w}}_{\widehat{\mathcal{S}}}, \widehat{\mathbf{C}}_{\widehat{\mathcal{S}}}) \prod_{i \notin \widehat{\mathcal{S}}} \delta(w_i). \quad (50)$$

Plugging the postulated PDF (38) in (37), one has

$$\begin{aligned} \mathcal{L}(q(\boldsymbol{\Omega}|\tilde{\mathbf{y}}); \widehat{\mathbf{s}}) &= \mathbb{E}_{q(\boldsymbol{\Omega}|\tilde{\mathbf{y}})} \left[ \frac{p(\tilde{\mathbf{y}}, \boldsymbol{\Omega}; \widehat{\mathbf{s}})}{q(\boldsymbol{\Omega}|\tilde{\mathbf{y}})} \right] \\ &= \mathbb{E}_{q(\boldsymbol{\Omega}|\tilde{\mathbf{y}})} \left[ \sum_{i=1}^N \ln p(s_i) + \ln p(\mathbf{w}|\mathbf{s}) + \ln p(\tilde{\mathbf{y}}|\boldsymbol{\theta}, \mathbf{w}) - \ln q(\mathbf{w}|\tilde{\mathbf{y}}) \right] + \text{const} \\ &= -\ln \det(\mathbf{J}_{\mathcal{S}} + \frac{1}{\tau} \mathbf{I}_{|\mathcal{S}|}) + \mathbf{h}_{\mathcal{S}}^H (\mathbf{J}_{\mathcal{S}} + \frac{1}{\tau} \mathbf{I}_{|\mathcal{S}|})^{-1} \mathbf{h}_{\mathcal{S}} \\ &\quad + \|\mathbf{s}\|_0 \ln \frac{\rho}{1-\rho} + \|\mathbf{s}\|_0 \ln \frac{1}{\tau} + \text{const} \\ &\triangleq \ln Z(\mathbf{s}) \end{aligned} \quad (51)$$

Then we need to find  $\hat{\mathbf{s}}$  which maximizes  $\ln Z(\mathbf{s})$ , i.e.,

$$\hat{\mathbf{s}} = \underset{\mathbf{s}}{\text{argmax}} \ln Z(\mathbf{s}). \quad (52)$$

The computation cost of enumerative method to find the globally optimal binary sequence  $\mathbf{s}$  of (52) is  $O(2^N)$ , which is impractical for typical values of  $N$ . In the Appendix VII-A, a greedy iterative search strategy similar to [19] is proposed. Since each step increases the objective function (which is bounded) and  $\mathbf{s}$  can take a finite number of values (at most  $2^N$ ), the method converges in a finite number of steps to some local optimum. In general, numerical experiments show that  $O(\hat{K})$  steps is often enough to find the local optimum.

Once  $\mathbf{s}$  is updated as  $\mathbf{s}'$ , the mean  $\widehat{\mathbf{w}}'_{\mathcal{S}'}$  and covariance  $\widehat{\mathbf{C}}'_{\mathcal{S}'}$  of the weights should be updated accordingly. For the active case,  $\widehat{\mathbf{w}}'_{\mathcal{S}'}$  and covariance  $\widehat{\mathbf{C}}'_{\mathcal{S}'}$  are updated according to (69) and (68), while for the deactive case,  $\widehat{\mathbf{w}}'_{\mathcal{S}'}$  and covariance  $\widehat{\mathbf{C}}'_{\mathcal{S}'}$  are updated according to (75) and (74).

3) *Estimating the model parameters:* After updating the frequencies and weights, the model parameters  $\boldsymbol{\beta} = \{\rho, \tau\}$  is estimated via maximizing the lower bound  $\mathcal{L}(q(\boldsymbol{\Omega}|\tilde{\mathbf{y}}); \boldsymbol{\beta})$  for fixed  $q(\boldsymbol{\Omega}|\tilde{\mathbf{y}})$ . Straightforward

calculation shows that

$$\begin{aligned}
\mathcal{L}(q(\boldsymbol{\Omega}|\tilde{\mathbf{y}}); \boldsymbol{\beta}) &= \mathbb{E}_{q(\boldsymbol{\Omega}|\tilde{\mathbf{y}})} \left[ \ln \frac{p(\tilde{\mathbf{y}}; \boldsymbol{\Omega}; \boldsymbol{\beta})}{q(\boldsymbol{\Omega}|\tilde{\mathbf{y}})} \right] \\
&= \mathbb{E}_{q(\boldsymbol{\Omega}|\tilde{\mathbf{y}})} \left[ \sum_{i=1}^N \ln p(s_i) + \ln p(\mathbf{w}|\mathbf{s}) \right] + \text{const} \\
&= \|\hat{\mathbf{s}}\|_0 \ln \rho + (N - \|\hat{\mathbf{s}}\|_0) \ln(1 - \rho) + \|\hat{\mathbf{s}}\|_0 \ln \frac{1}{\pi\tau} - \mathbb{E}_{q(\mathbf{w}|\tilde{\mathbf{y}})} \left[ \frac{1}{\tau} \mathbf{w}_{\hat{\mathcal{S}}}^H \mathbf{w}_{\hat{\mathcal{S}}} \right] + \text{const}. \tag{53}
\end{aligned}$$

Because

$$\mathbb{E}_{q(\mathbf{w}|\tilde{\mathbf{y}})} [\mathbf{w}_{\hat{\mathcal{S}}}^H \mathbf{w}_{\hat{\mathcal{S}}}] = \mathbb{E}_{q(\mathbf{w}|\tilde{\mathbf{y}})} \left[ \sum_{i \in \hat{\mathcal{S}}} w_i^* w_i \right] = \hat{\mathbf{w}}_{\hat{\mathcal{S}}}^H \hat{\mathbf{w}}_{\hat{\mathcal{S}}} + \text{tr}(\hat{\mathbf{C}}_{\hat{\mathcal{S}}}),$$

we obtain

$$\mathcal{L}(q(\boldsymbol{\Omega}|\tilde{\mathbf{y}}); \boldsymbol{\beta}) = -\frac{1}{\tau} [(\hat{\mathbf{w}}_{\hat{\mathcal{S}}}^H \hat{\mathbf{w}}_{\hat{\mathcal{S}}}) + \text{tr}(\hat{\mathbf{C}}_{\hat{\mathcal{S}}})] + p \|\hat{\mathbf{s}}\|_0 \left( \ln \frac{\rho}{1 - \rho} - \ln \tau \right) + N \ln(1 - \rho) + \text{const}.$$

Setting  $\frac{\partial \mathcal{L}}{\partial \rho} = 0$ ,  $\frac{\partial \mathcal{L}}{\partial \tau} = 0$ , we have

$$\begin{aligned}
\hat{\rho} &= \frac{\|\hat{\mathbf{s}}\|_0}{N}, \\
\hat{\tau} &= \frac{\hat{\mathbf{w}}_{\hat{\mathcal{S}}}^H \hat{\mathbf{w}}_{\hat{\mathcal{S}}} + \text{tr}(\hat{\mathbf{C}}_{\hat{\mathcal{S}}})}{\|\hat{\mathbf{s}}\|_0}. \tag{54}
\end{aligned}$$

4) *Summary of the VALSE algorithm:* Now the VALSE algorithm is summarized as Algorithm 1 for completeness. Let  $\hat{\mathcal{S}}$  be the estimate of  $\mathcal{S}$  by the VALSE algorithm. Note that for the first outer iteration, the VALSE is initialized using the noncoherent estimation [19, subsection E of Section IV]. For the outer iteration greater than 1, VALSE is initialized with the previous results.

---

**Algorithm 1** Outline of VALSE algorithm [19].

---

**Input:** Signal vector  $\tilde{\mathbf{y}}$ , noise variance  $\tilde{\sigma}^2$

**Output:** The model order estimate  $\hat{K}$ , frequencies posterior PDF  $q(\theta_i|\tilde{\mathbf{y}})$ ,  $i \in \hat{\mathcal{S}}$ , complex weights estimate  $\hat{\mathbf{w}}_{\hat{\mathcal{S}}}$  and covariance matrix  $\hat{\mathbf{C}}_{\hat{\mathcal{S}}}$ , and reconstructed signal  $\hat{\mathbf{z}}$

- 1: Initialize  $\hat{\rho}, \hat{\tau}$  and  $q_{\theta_i|\tilde{\mathbf{y}}}$ ,  $i \in \{1, \dots, N\}$ ; compute  $\hat{\mathbf{a}}_i$
  - 2: **repeat**
  - 3:   Update  $\hat{\mathbf{s}}, \hat{\mathbf{w}}_{\hat{\mathcal{S}}}$  and  $\hat{\mathbf{C}}_{\hat{\mathcal{S}}}$  (Section IV-B2)
  - 4:   Update  $\hat{\rho}, \hat{\tau}$  (54)
  - 5:   Update  $\boldsymbol{\eta}_i$  and  $\hat{\mathbf{a}}_i$  for all  $i \in \hat{\mathcal{S}}$  (Section IV-B1)
  - 6: **until** stopping criterion is satisfied
  - 7: **return**  $\hat{K}, \hat{\boldsymbol{\theta}}_{\hat{\mathcal{S}}}, \hat{\mathbf{w}}_{\hat{\mathcal{S}}}, \hat{\mathbf{C}}_{\hat{\mathcal{S}}}$  and  $\hat{\mathbf{z}}$
-

### C. From VALSE module to MMSE module

According to the approximated posterior PDF  $q(\mathbf{w}_{\hat{\mathcal{S}}|\tilde{\mathbf{y}}})$  and  $q(\boldsymbol{\theta}|\tilde{\mathbf{y}})$ , we calculate the message  $m_{\delta \rightarrow \mathbf{z}}^{t+1}(\mathbf{z})$  as

$$m_{\delta \rightarrow \mathbf{z}}^{t+1}(\mathbf{z}) \propto \frac{\text{Proj}[\int q(\mathbf{w}_{\hat{\mathcal{S}}|\tilde{\mathbf{y}}})\delta(\mathbf{z} - \mathbf{A}_{\hat{\mathcal{S}}}(\boldsymbol{\theta})\mathbf{w}_{\hat{\mathcal{S}}})q(\boldsymbol{\theta}|\tilde{\mathbf{y}})d\mathbf{w}_{\hat{\mathcal{S}}}d\boldsymbol{\theta}]}{m_{\mathbf{z} \rightarrow \delta}^t(\mathbf{z})} \triangleq \frac{\text{Proj}[q_{\mathbf{A}}^{t+1}(\mathbf{z})]}{m_{\mathbf{z} \rightarrow \delta}^t(\mathbf{z})}. \quad (55)$$

Then we calculate the posterior means and variances of  $\mathbf{z}$  averaged over  $q_{\mathbf{A}}^{t+1}(\mathbf{z})$  as

$$\mathbf{z}_{\mathbf{A}}^{\text{post}} = \hat{\mathbf{A}}_{\hat{\mathcal{S}}}\hat{\mathbf{w}}_{\hat{\mathcal{S}}}, \quad (56)$$

$$\begin{aligned} \mathbf{v}_{\mathbf{A}}^{\text{post}} &= \text{diag}(\hat{\mathbf{A}}_{\hat{\mathcal{S}}}\hat{\mathbf{C}}_{\hat{\mathcal{S}}}\hat{\mathbf{A}}_{\hat{\mathcal{S}}}^H) + \left(\hat{\mathbf{w}}_{\hat{\mathcal{S}}}^H\hat{\mathbf{w}}_{\hat{\mathcal{S}}}\mathbf{1}_M - |\hat{\mathbf{A}}_{\hat{\mathcal{S}}}|^2|\hat{\mathbf{w}}_{\hat{\mathcal{S}}}|^2\right) \\ &+ \left[\text{tr}(\hat{\mathbf{C}}_{\hat{\mathcal{S}}})\mathbf{1}_M - |\hat{\mathbf{A}}_{\hat{\mathcal{S}}}|^2\text{diag}(\hat{\mathbf{C}}_{\hat{\mathcal{S}}})\right], \end{aligned} \quad (57)$$

where details of calculating (57) is postponed to Appendix VII-B. Thus  $\text{Proj}[q_{\mathbf{A}}^{t+1}(\mathbf{z})]$  is

$$\text{Proj}[q_{\mathbf{A}}^{t+1}(\mathbf{z})] = \mathcal{CN}(\mathbf{z}; \mathbf{z}_{\mathbf{A}}^{\text{post}}, \text{diag}(\mathbf{v}_{\mathbf{A}}^{\text{post}})). \quad (58)$$

According to (55),  $m_{\delta \rightarrow \mathbf{z}}^{t+1}(\mathbf{z})$  is calculated to be

$$m_{\delta \rightarrow \mathbf{z}}^{t+1}(\mathbf{z}) = \mathcal{CN}(\mathbf{z}; \mathbf{z}_{\mathbf{A}}^{\text{ext}}(t+1), \text{diag}(\mathbf{v}_{\mathbf{A}}^{\text{ext}}(t+1))), \quad (59)$$

where the extrinsic  $\mathbf{z}_{\mathbf{A}}^{\text{ext}}(t+1)$  and variance  $\mathbf{v}_{\mathbf{A}}^{\text{ext}}(t+1)$  are given by [38]

$$\frac{1}{\mathbf{v}_{\mathbf{A}}^{\text{ext}}(t+1)} = \frac{1}{\mathbf{v}_{\mathbf{A}}^{\text{post}}(t)} - \frac{1}{\tilde{\boldsymbol{\sigma}}_w^2(t)}, \quad (60)$$

$$\mathbf{z}_{\mathbf{A}}^{\text{ext}}(t+1) = \mathbf{v}_{\mathbf{A}}^{\text{ext}}(t+1) \odot \left( \frac{\mathbf{z}_{\mathbf{A}}^{\text{post}}(t)}{\mathbf{v}_{\mathbf{A}}^{\text{post}}(t)} - \frac{\tilde{\mathbf{y}}(t)}{\tilde{\boldsymbol{\sigma}}_w^2(t)} \right), \quad (61)$$

and we input them to module B. The algorithm iterates until convergence or the maximum number of iterations is reached. It is worth noting that for unquantized system, VALSE-EP is reduced to the VALSE algorithm. The VALSE-EP algorithm is summarized as Algorithm 2.

### D. Implementation Details

To implement the VALSE algorithm, several strategies are proposed to improve the robustness of the proposed algorithm:

- The extrinsic variances  $v_{\mathbf{A}}^{\text{ext}}$  and  $v_{\mathbf{B}}^{\text{ext}}$  are restricted to the interval  $[v_{\min}, v_{\max}]$ . Here  $v_{\min} = 10^{-8}$  and  $v_{\max} = 10^8$ .
- For the first iteration, the VALSE algorithm is initialized the same as [19]. After the first iteration, warm start is adopted and the VALSE is initialized with the previous results. In details,  $\mathbf{J}$ ,  $\mathbf{h}$ ,  $\rho$ ,  $\tau$ ,  $\mathbf{s}$ ,  $\mathbf{A}$ ,  $\mathbf{C}$ ,  $\mathbf{w}$  are initialized with the previous results.

---

**Algorithm 2** VALSE-EP algorithm
 

---

- 1: Initialize  $\mathbf{v}_A^{\text{ext}}(1) = \mathbf{10}^4$ ,  $\mathbf{z}_A^{\text{ext}}(1) = \mathbf{0}_M$ ; Set the number of outer iterations  $T_{\text{outer}}$ ;
  - 2: **for**  $t = 1, \dots, T_{\text{outer}}$  **do**
  - 3:   Compute the post mean and variance of  $\mathbf{z}$  as  $\mathbf{z}_B^{\text{post}}(t)$  (28),  $\mathbf{v}_B^{\text{post}}(t)$  (29).
  - 4:   Compute the extrinsic mean and variance of  $\mathbf{z}$  as  $\mathbf{z}_B^{\text{ext}}(t)$  (32b) and  $\mathbf{v}_B^{\text{ext}}(t)$  (32a), and set  $\tilde{\sigma}^2(t) = \mathbf{v}_B^{\text{ext}}(t)$  and  $\tilde{\mathbf{y}}(t) = \mathbf{z}_B^{\text{ext}}(t)$ .
  - 5:   If  $t = 1$ , initialize  $\rho, \tau, q(\theta_i|\tilde{\mathbf{y}})$ ,  $i = 1, \dots, N$  and compute  $\hat{\mathbf{A}}$  using  $\tilde{\mathbf{y}}(t)$ . Then run the VALSE algorithm 1 until the stopping criterion is satisfied. Otherwise, run the VALSE algorithm 1 directly with initialization provided by the previous results of the VALSE.
  - 6:   Calculate the posterior means  $\mathbf{z}_A^{\text{post}}(t)$  (56) and variances  $\mathbf{v}_A^{\text{post}}(t)$  (57).
  - 7:   Compute the extrinsic mean and variance of  $\mathbf{z}$  as  $\mathbf{v}_A^{\text{ext}}(t+1)$  (60),  $\mathbf{z}_A^{\text{ext}}(t+1)$  (61).
  - 8: **end for**
  - 9: Return  $\hat{\boldsymbol{\theta}}, \hat{\mathbf{w}}, \hat{\mathbf{z}}$  and  $\hat{K}$ .
- 

### E. Computation Complexity

In [19], it shows that the complexity per iteration of the VALSE is dominated by the two steps: the maximization of  $\ln Z(\mathbf{s})$  and the approximations of the posterior PDF  $q(\theta_i|\mathbf{y})$  by mixtures of von Mises pdfs. This work approximates the posterior PDF  $q(\theta_i|\mathbf{y})$  by Heuristic 2 in [19, Algorithm 2]. Thus the complexity of the two steps are  $O(NK^3)$  and  $O(MN)$  [19]. For a single iteration, the computation complexity of VALSE-EP is  $O(MN + NK^3)$ . For the VALSE-EP algorithm, the computation is dominated by the VALSE algorithm. Thus the VALSE-EP is comparable to that of the VALSE for a single outer iteration. Compared to the atomic norm based algorithm, the computation complexity is  $O(M^{6.5})$  [17]. Since  $N$  and  $M$  are usually the same order, the computation complexity of the VALSE-EP is significantly lower than that of the atomic norm based algorithm.

## V. NUMERICAL SIMULATION

In this section, numerical experiments are conducted to verify the proposed algorithm. We evaluate the signal estimation error, frequency estimation error, the correct model order estimation probability under quantized measurements.

The frequencies are randomly drawn such that the minimum wrap around distance is greater than  $2\pi/N$ . We evaluate the performance of the VALSE algorithm utilizing noninformative prior, i.e.,  $p(\theta_i) = 1/(2\pi)$ ,  $i = 1, \dots, N$ . The magnitudes of the weight coefficients are drawn i.i.d. from a Gaussian distribution  $\mathcal{N}(1, 0.04)$ , and the phases are drawn i.i.d. from a uniform distribution between  $[-\pi, \pi]$ .

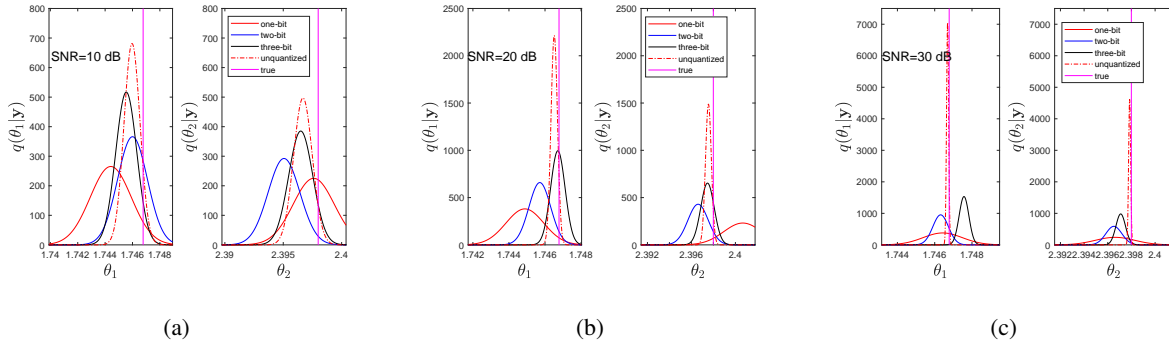


Fig. 3. The posterior PDF  $q(\theta_i|\tilde{\mathbf{y}})$  output by the VALSE-EP. Here we set  $K = 2$ ,  $N = 100$ ,  $M = 60$ , and the true frequencies are  $[\theta_1, \theta_2] = [1.7468, 2.3980]$ . Note that the red line, blue line, black line and the dashed red line denote the posterior PDF from one-bit, two-bit, three-bit and unquantized observations, and the vertical magenta line denotes the true frequency.

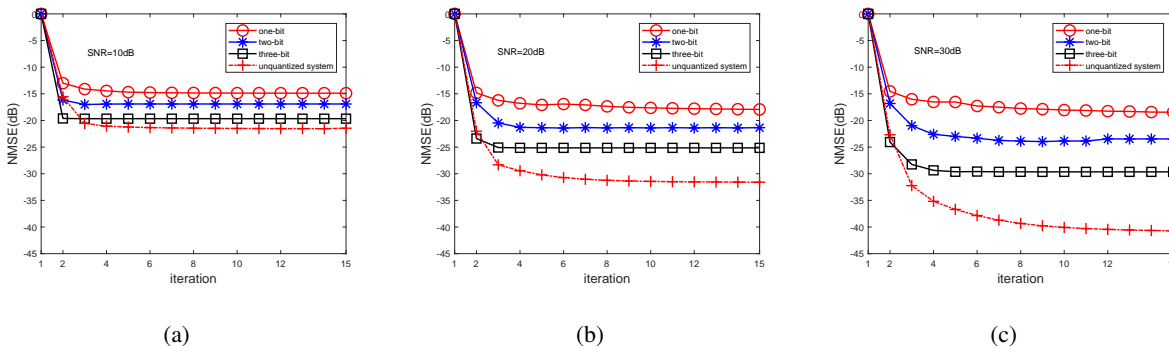


Fig. 4. The NMSE of the LSE of the VALSE-EP versus the number of iterations under SNR = 10 dB, SNR = 20 dB, SNR = 30 dB, respectively. Here we set  $N = 100$ ,  $M = 60$ ,  $K = 3$  and the results are averaged over 50 MC trials.

For multi-bit quantization, a uniform quantizer is adopted and the quantization interval is restricted to  $[-3\sigma_z, 3\sigma_z]$ , where  $\sigma_z^2$  is the variance of the signal  $\Re\{\mathbf{z}_N\}$  or  $\Im\{\mathbf{z}_N\}$ . In our setting, it can be calculated that  $\sigma_z^2 \approx K/2$ . For one-bit quantization, zero is chosen as the threshold. We define the SNR as  $\text{SNR} = 20\log(\|\mathbf{A}(\boldsymbol{\theta})\mathbf{w}\|_2/\|\mathbf{n}\|_2)$ .

The number of maximum outer iterations is set as  $T_{\text{outer}} = 100$ . As for the inner VALSE algorithm provided by [19], the parameters are kept unchanged.

The normalized MSE (NMSE) of signal  $\hat{\mathbf{z}}$  (for unquantized and multi-bit quantized system) and  $\hat{\boldsymbol{\theta}}$  are defined as  $20\log(\|\hat{\mathbf{z}} - \mathbf{z}\|_2/\|\mathbf{z}\|_2)$  and  $20\log(\|\hat{\boldsymbol{\theta}} - \boldsymbol{\theta}\|_2)$ , respectively. Please note that, due to magnitude ambiguity, it is impossible to recover the exact magnitude of  $\tilde{w}_k$  from one-bit measurements in the noiseless scenario. Thus for one-bit quantization, the debiased NMSE of the signal defined as  $\min_c 10\log(\|\mathbf{z}^* - c\hat{\mathbf{z}}\|_2/\|\mathbf{z}^*\|_2)$  are calculated. As for the frequency estimation error, we average only

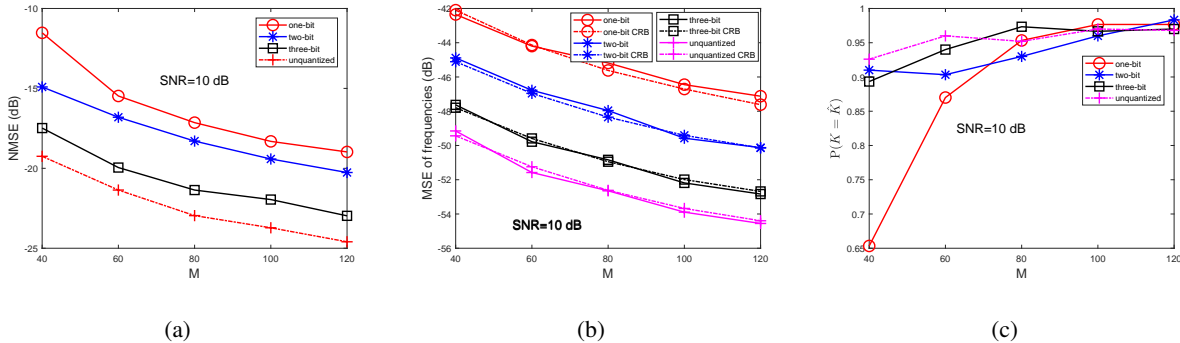


Fig. 5. The performance of the VALSE-EP versus the number of measurements. Here we set  $N = 120$ ,  $K = 3$ ,  $\text{SNR} = 10$  dB.

the trials in which all those algorithms estimate the correct model order. All the results are averaged over 300 Monte Carlo (MC) trials unless stated otherwise. The model order is correctly estimated only when both  $\hat{K} = K$  and  $\text{NMSE}(\mathbf{z}) \leq -10\text{dB}$  are satisfied. The empirical probability of correct model order estimation  $P(\hat{K} = K)$  is adopted as a performance metric. The MSE of the frequency estimation is calculated only when the model order is correctly estimated.

At first, an experiment is conducted to plot the posterior PDF of the frequencies  $q(\theta_i|\mathbf{y})$ . The results are averaged over 50 MC trials and is presented in Fig. 3. For each trial, the posterior PDF of the frequency  $q(\theta_i|\mathbf{y})$  is approximated as a von Mises distribution  $\mathcal{VM}(\theta_i, \mu_i, \kappa_i)$ , where  $\mu_i$  and  $\kappa_i$  are the mean and concentration parameters. Since the precision is approximately  $\kappa_i$  for the von Mises distribution  $\mathcal{VM}(\theta_i, \mu_i, \kappa_i)$  when  $\kappa_i$  is large [46], the arithmetic mean of the mean parameter and the concentration parameter are obtained as the average of the MC trials. It can be seen that the mean of the posterior PDF is close to the true frequency. In addition, as the bit-depth or the SNR increases, the posterior PDF of the frequencies  $q(\theta_i|\mathbf{y})$  become more peaked, and thus more concentrated, which implies that the uncertain degrees becomes smaller.

#### A. NMSE of the line spectral versus the iteration

The NMSEs of the line spectral versus the iteration are investigated. The results are averaged over 50 MC trials. Note that the VALSE-EP converges in tens of iterations. Meanwhile, the LSE signal can be recovered from one-bit samples. The performance of the VALSE-EP improves as SNR increases, especially for higher bit-depth. As the bit-depth increases, the performance of the VALSE-EP approaches to that of the VALSE algorithm.

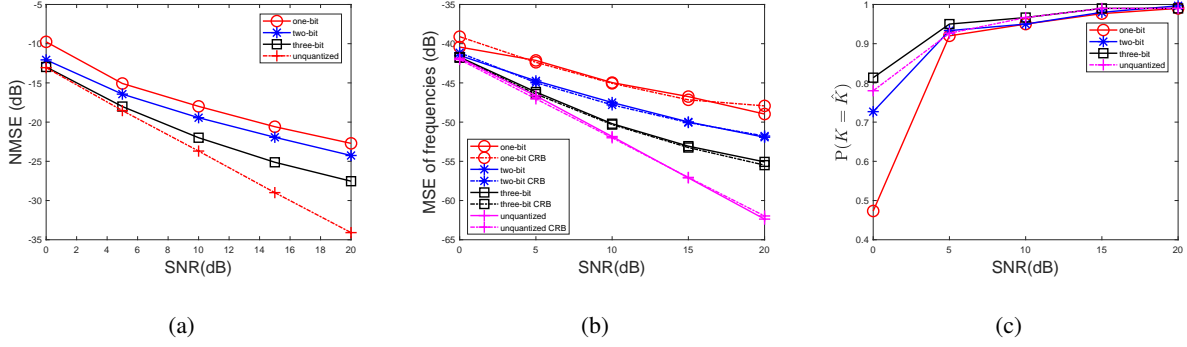


Fig. 6. The performance of the VALSE-EP versus SNR. Here we set  $N = M = 100$  and  $K = 3$ .

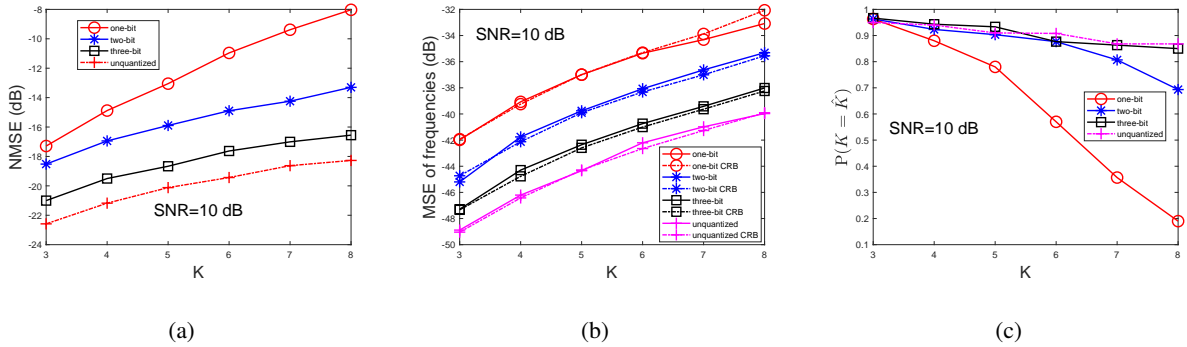


Fig. 7. The performance of the VALSE-EP versus the number of spectrum  $K$ . Here we set  $N = M = 80$  and  $\text{SNR} = 10$  dB.

### B. Estimation by varying $M$

We examine the performance of the VALSE-EP by varying the number of measurements  $M$ . The results are shown in Fig. 5. It can be seen that both the NMSE of the LSE and the frequency estimation error decreases as the number of measurements  $M$  increases. In addition, the frequency estimation error is close to the CRB. As the number of measurements  $M$  increases, the probability of correct model order estimation increases. In summary, the performances of the VALSE-EP improves as  $M$  increases.

### C. Estimation by varying SNR

The performance of the VALSE-EP with varied SNR is investigated and the results are plotted in Fig. 6. It can be seen that as SNR increases, the NMSE of the LSE decreases. In addition, the MSE of the frequency estimation decreases and is close to the CRB. The correct model order estimation probability increases as SNR increases.

#### D. Estimation by varying $K$

Here the performance of the VALSE-EP is investigated with respect to the number of spectrum  $K$ , and the results are presented in Fig. 7. From Fig. 7(a) and Fig. 7(b), it can be seen that as the number of spectrum  $K$  increases, the NMSE and the MSE of the frequencies increases. From Fig. 7(c), the correct model order estimation probability decreases as the number of spectrum  $K$  increases, especially for the one-bit and two-bit scenarios. It is worth noting that the MSE of the frequencies is close to the CRB, except for one-bit measurements when  $K \geq 7$ . The reason may be that the correct model order estimation probability from the one-bit measurements is too low and the number of trials for averaging is not enough.

### VI. CONCLUSION

In this paper, a VALSE-EP algorithm is proposed to deal with the fundamental LSE problem from quantized samples. The VALSE-EP is a grid-less algorithm which iteratively refines the frequency estimates, automatically estimates the model order, learns the parameters of the prior distribution, and has a low computation complexity. In addition, the VALSE-EP provides the uncertain degrees of the frequency estimates from quantized samples. Finally, substantial numerical experiments are conducted to show the excellent performance of the VALSE-EP.

### VII. APPENDIX

#### A. Finding the local maximum of $\ln Z(\mathbf{s})$

A greedy iterative search strategy similar to [19] is adopted to find a local maximum of  $\ln Z(\mathbf{s})$ . We proceed as follows: In the  $p$ th iteration, the  $k$ th test sequence  $\mathbf{t}_k$  which flips the  $k$ th element of  $\mathbf{s}^{(p)}$  is obtained. Then  $\Delta_k^{(p)} = \ln Z(\mathbf{t}_k) - \ln Z(\mathbf{s}^{(p)})$  is calculated for each  $k = 1, \dots, N$ . If  $\Delta_k^{(p)} < 0$  holds for all  $k$ , the algorithm is terminated and  $\hat{\mathbf{s}}$  is set as  $\mathbf{s}^{(p)}$ , otherwise  $t_k$  corresponding to the maximum  $\Delta_k^{(p)}$  is chosen as  $\mathbf{s}^{(p+1)}$  in the next iteration.

When  $k \notin \mathcal{S}$ , that is,  $s_k = 0$ , we activate the  $k$ th component of  $\mathbf{s}$  by setting  $s'_k = 1$ . Now,  $\mathcal{S}' = \mathcal{S} \cup \{k\}$ .

$$\begin{aligned}
 \Delta_k &= \ln Z(\mathbf{s}') - \ln Z(\mathbf{s}) \\
 &= \ln \det(\mathbf{J}_{\mathcal{S}} + \frac{1}{\tau} \mathbf{I}_{|\mathcal{S}|}) - \ln \det(\mathbf{J}_{\mathcal{S}'} + \frac{1}{\tau} \mathbf{I}_{|\mathcal{S}'|}) \\
 &\quad + \ln \frac{\rho}{1-\rho} + \ln \frac{1}{\tau} + \mathbf{h}_{\mathcal{S}'}^H (\mathbf{J}_{\mathcal{S}'} + \frac{1}{\tau} \mathbf{I}_{|\mathcal{S}'|})^{-1} \mathbf{h}_{\mathcal{S}'} \\
 &\quad - \mathbf{h}_{\mathcal{S}}^H (\mathbf{J}_{\mathcal{S}} + \frac{1}{\tau} \mathbf{I}_{|\mathcal{S}|})^{-1} \mathbf{h}_{\mathcal{S}}.
 \end{aligned} \tag{62}$$

Let  $\mathbf{j}_k$  be  $\mathbf{j}_k = [J_{ik}|i \in \mathcal{S}]^T$ . By using the block-matrix determinant formula, one has

$$\begin{aligned} \ln(\det(\mathbf{J}_{\mathcal{S}'} + \frac{1}{\tau}\mathbf{I}_{|\mathcal{S}'|})) &= \ln \det(\mathbf{J}_{\mathcal{S}} + \frac{1}{\tau}\mathbf{I}_{|\mathcal{S}|}) \\ &+ \ln\left(\text{tr}(\boldsymbol{\Sigma}^{-1}) + \frac{1}{\tau} - \mathbf{j}_k^H(\mathbf{J}_{\mathcal{S}} + \frac{1}{\tau}\mathbf{I}_{|\mathcal{S}|})^{-1}\mathbf{j}_k\right), \end{aligned} \quad (63)$$

By the block-wise matrix inversion formula, one has

$$\begin{aligned} \mathbf{h}_{\mathcal{S}'}^H(\mathbf{J}_{\mathcal{S}'} + \frac{1}{\tau}\mathbf{I}_{|\mathcal{S}'|})^{-1}\mathbf{h}_{\mathcal{S}'} &= \mathbf{h}_{\mathcal{S}}^H(\mathbf{J}_{\mathcal{S}} + \frac{1}{\tau}\mathbf{I}_{|\mathcal{S}|})^{-1}\mathbf{h}_{\mathcal{S}} \\ &+ \frac{q^*q}{\text{tr}(\boldsymbol{\Sigma}^{-1}) + \frac{1}{\tau} - \mathbf{j}_k^H(\mathbf{J}_{\mathcal{S}} + \frac{1}{\tau}\mathbf{I}_{|\mathcal{S}|})^{-1}\mathbf{j}_k}, \end{aligned} \quad (64)$$

where  $q = h_k - \mathbf{j}_k^H(\mathbf{J}_{\mathcal{S}} + \frac{1}{\tau}\mathbf{I}_{|\mathcal{S}|})^{-1}\mathbf{h}_{\mathcal{S}}$ . Plugging (63) and (64) in (62), and let

$$\begin{aligned} v_k &= \left(\text{tr}(\boldsymbol{\Sigma}^{-1}) + \frac{1}{\tau} - \mathbf{j}_k^H(\mathbf{J}_{\mathcal{S}} + \frac{1}{\tau}\mathbf{I}_{|\mathcal{S}|})^{-1}\mathbf{j}_k\right)^{-1} \text{ and} \\ u_k &= v_k \left(h_k - \mathbf{j}_k^H(\mathbf{J}_{\mathcal{S}} + \frac{1}{\tau}\mathbf{I}_{|\mathcal{S}|})^{-1}\mathbf{h}_{\mathcal{S}}\right), \end{aligned} \quad (65)$$

$\Delta_k$  can be simplified as

$$\Delta_k = \ln \frac{v_k}{\tau} + \frac{|u_k|^2}{v_k} + \ln \frac{\rho}{1-\rho}. \quad (66)$$

Given that  $\mathbf{s}$  is changed into  $\mathbf{s}'$ , the mean  $\widehat{\mathbf{w}}'_{\mathcal{S}'}$  and covariance  $\widehat{\mathbf{C}}'_{\mathcal{S}'}$  of the weights can be updated from (49), i.e.,

$$\widehat{\mathbf{C}}'_{\mathcal{S}'} = (\mathbf{J}_{\mathcal{S}'} + \frac{1}{\tau}\mathbf{I}_{|\mathcal{S}'|})^{-1}, \quad (67a)$$

$$\widehat{\mathbf{w}}'_{\mathcal{S}'} = \widehat{\mathbf{C}}'_{\mathcal{S}'}\mathbf{h}_{\mathcal{S}'}. \quad (67b)$$

In fact, the matrix inversion can be avoided when updating  $\widehat{\mathbf{w}}'_{\mathcal{S}'}$  and  $\widehat{\mathbf{C}}'_{\mathcal{S}'}$ . It can be shown that

$$\begin{aligned} \widehat{\mathbf{C}}'_{\mathcal{S}'} &= \begin{pmatrix} \widehat{\mathbf{C}}'_{\mathcal{S}' \setminus k} & \widehat{\mathbf{c}}'_k \\ \widehat{\mathbf{c}}_k^H & \widehat{C}'_{kk} \end{pmatrix} = (\mathbf{J}_{\mathcal{S}'} + \frac{1}{\tau}\mathbf{I}_{|\mathcal{S}'|})^{-1} \\ &= \begin{pmatrix} \widehat{\mathbf{C}}_{\mathcal{S}} & \mathbf{0} \\ \mathbf{0} & 0 \end{pmatrix} + v_k \begin{pmatrix} \widehat{\mathbf{C}}_{\mathcal{S}}\mathbf{j}_k \\ -1 \end{pmatrix} \begin{pmatrix} \widehat{\mathbf{C}}_{\mathcal{S}}\mathbf{j}_k \\ -1 \end{pmatrix}^H, \\ &= \begin{pmatrix} \widehat{\mathbf{C}}_{\mathcal{S}} + v_k\widehat{\mathbf{C}}_{\mathcal{S}}\mathbf{j}_k(\widehat{\mathbf{C}}_{\mathcal{S}}\mathbf{j}_k)^H & -v_k\widehat{\mathbf{C}}_{\mathcal{S}}\mathbf{j}_k \\ -v_k(\widehat{\mathbf{C}}_{\mathcal{S}}\mathbf{j}_k)^H & v_k \end{pmatrix} \end{aligned} \quad (68)$$

$\widehat{\mathbf{C}}'_{S'}$  is obtained if  $\widehat{\mathbf{c}}'_k$ ,  $\widehat{\mathbf{c}}_k^H$  and  $\widehat{C}'_{kk}$  are inserted appropriately in  $\widehat{\mathbf{C}}'_{S'\setminus k}$ , and

$$\begin{aligned}\widehat{\mathbf{w}}'_{S'} &= \begin{pmatrix} \widehat{\mathbf{w}}'_{S'\setminus k} \\ \widehat{w}'_k \end{pmatrix} = \widehat{\mathbf{C}}_{S'} \mathbf{h}_{S'} \\ &= \begin{pmatrix} \widehat{\mathbf{C}}_S \mathbf{h}_S + v_k \widehat{\mathbf{C}}_S \mathbf{j}_k \mathbf{j}_k^H \widehat{\mathbf{C}}_S \mathbf{h}_S - v_k \widehat{\mathbf{C}}_S \mathbf{j}_k h_k \\ -v_k \mathbf{j}_k^H \widehat{\mathbf{C}}_S \mathbf{h}_S + v_k h_k \end{pmatrix} \\ &= \begin{pmatrix} \widehat{\mathbf{C}}_S \mathbf{h}_S - u_k \widehat{\mathbf{C}}_S \mathbf{j}_k \\ u_k \end{pmatrix}.\end{aligned}\quad (69)$$

From (69) and (68), one can see that after activating the  $k$ th component, the posterior mean and variance of  $w_k$  are  $u_k$  and  $v_k$ , respectively.

For the deactive case with  $s_k = 1$ ,  $s'_k = 0$  and  $S' = S \setminus \{k\}$ ,  $\Delta_k = \ln Z(\mathbf{s}') - \ln Z(\mathbf{s})$  is the negative of (66), i.e.,

$$\Delta_k = -\ln \frac{v_k}{\tau} - \frac{|u_k|^2}{v_k} - \ln \frac{\rho}{1-\rho}.\quad (70)$$

Similar to (68), the posterior mean and covariance update equation from  $S'$  to  $S$  case can be rewritten as

$$\begin{pmatrix} \widehat{\mathbf{C}}'_{S'} & \mathbf{0} \\ \mathbf{0} & 0 \end{pmatrix} + v_k \begin{pmatrix} \widehat{\mathbf{C}}'_{S'} \mathbf{j}_k \\ -1 \end{pmatrix} \begin{pmatrix} \widehat{\mathbf{C}}'_{S'} \mathbf{j}_k \\ -1 \end{pmatrix}^H = \begin{pmatrix} \widehat{\mathbf{C}}_{S\setminus k} & \widehat{\mathbf{c}}_k \\ \widehat{\mathbf{c}}_k^H & \widehat{C}_{kk} \end{pmatrix},\quad (71)$$

and

$$\begin{pmatrix} \widehat{\mathbf{w}}'_{S'} - u_k \widehat{\mathbf{C}}'_{S'} \mathbf{j}_k \\ u_k \end{pmatrix} = \begin{pmatrix} \widehat{\mathbf{C}}'_{S'} \mathbf{h}_{S'} - u_k \widehat{\mathbf{C}}'_{S'} \mathbf{j}_k \\ u_k \end{pmatrix} = \begin{pmatrix} \widehat{\mathbf{w}}_{S\setminus k} \\ \widehat{w}_k \end{pmatrix},\quad (72)$$

where  $\widehat{\mathbf{c}}_{k,0}$  denotes the column of  $\widehat{\mathbf{C}}_{S,0}$  corresponding to the  $k$ th component. According to (71) and (72), one has

$$\widehat{\mathbf{C}}'_{S'} + v_k \widehat{\mathbf{C}}'_{S'} \mathbf{j}_k \mathbf{j}_k^H \widehat{\mathbf{C}}'_{S'} = \widehat{\mathbf{C}}_{S\setminus k},\quad (73a)$$

$$-v_k \widehat{\mathbf{C}}'_{S'} \mathbf{j}_k = \widehat{\mathbf{c}}_k\quad (73b)$$

$$v_k = \widehat{C}_{kk},\quad (73c)$$

$$\widehat{\mathbf{w}}'_{S'} - u_k \widehat{\mathbf{C}}'_{S'} \mathbf{j}_k = \widehat{\mathbf{w}}_{S\setminus k},\quad (73d)$$

$$u_k = \widehat{w}_k.\quad (73e)$$

Thus,  $\widehat{\mathbf{C}}'_{S'}$  can be updated by substituting (73b) and (73c) in (73a), i.e.,

$$\widehat{\mathbf{C}}'_{S'} = \widehat{\mathbf{C}}_{S\setminus k} - v_k \widehat{\mathbf{C}}'_{S'} \mathbf{j}_k \mathbf{j}_k^H \widehat{\mathbf{C}}'_{S'} = \widehat{\mathbf{C}}_{S\setminus k} - \frac{\widehat{\mathbf{c}}_k \widehat{\mathbf{c}}_k^H}{\widehat{C}_{kk}}.\quad (74)$$

Similarly,  $\widehat{\mathbf{w}}'_{\mathcal{S}'}$  can be updated by substituting (73b) and (73e) in (73d), i.e.,

$$\widehat{\mathbf{w}}'_{\mathcal{S}'} = u_k \widehat{\mathbf{C}}'_{\mathcal{S}'} \mathbf{j}_k + \widehat{\mathbf{w}}_{\mathcal{S}' \setminus k} = \widehat{\mathbf{w}}_{\mathcal{S}' \setminus k} - \frac{\widehat{w}_k}{\widehat{C}_{kk}} \widehat{\mathbf{c}}_k. \quad (75)$$

According to  $v_k = \widehat{C}_{kk}$  (73c) and  $u_k = \widehat{w}_k$  (73e),  $\Delta_k$  (70) can be simplified as

$$\Delta_k = -\ln \frac{\widehat{C}_{kk}}{\tau} - \frac{|w_k|^2}{\widehat{C}_{kk}} - \ln \frac{\rho}{1 - \rho}. \quad (76)$$

### B. Calculating the post variance $\mathbf{v}_A^{\text{post}}$ (57) of $\mathbf{z}$

Now we calculate the variance of  $z_i$  given  $q(\mathbf{w}_{\hat{\mathcal{S}}}|\tilde{\mathbf{y}})$  and  $q(\boldsymbol{\theta}|\tilde{\mathbf{y}})$ . Let  $\mathbf{b}_i^T = [e^{jm_i\theta_1}, e^{jm_i\theta_2}, \dots, e^{jm_i\theta_K}]$  be the  $i$ th row of  $\mathbf{A}_{\hat{\mathcal{S}}}$ . Then  $z_i = \mathbf{b}_i^T \mathbf{w}_{\hat{\mathcal{S}}}$ . The variance is

$$\begin{aligned} \text{Var}[z_i] &= \text{E}[|z_i|^2] - |\text{E}[z_i]|^2 = \text{E}[|\mathbf{b}_i^T \mathbf{w}_{\hat{\mathcal{S}}}|^2] - |\text{E}[\mathbf{b}_i^T \mathbf{w}_{\hat{\mathcal{S}}}]|^2 \\ &= \text{tr} \left[ (\mathbf{C}_{\hat{\mathcal{S}}} + \widehat{\mathbf{w}}_{\hat{\mathcal{S}}} \widehat{\mathbf{w}}_{\hat{\mathcal{S}}}^H) \text{E}[\mathbf{b}_i^* \mathbf{b}_i^T] \right] - |\widehat{\mathbf{b}}_i^T \widehat{\mathbf{w}}_{\hat{\mathcal{S}}}|^2. \end{aligned} \quad (77)$$

where

$$\text{E}[\mathbf{b}_i^* \mathbf{b}_i^T] = \widehat{\mathbf{b}}_i^* \widehat{\mathbf{b}}_i^T + \text{diag} \left( \mathbf{1}_M - |\widehat{\mathbf{b}}_i|^2 \right). \quad (78)$$

Substituting (78) in (77), one obtains (57).

## REFERENCES

- [1] W. Bajwa, A. Sayeed, and R. Nowak, "Compressed channel sensing: A new approach to estimating sparse multipath channels," *Proc. IEEE*, vol. 98, pp. 1058-1076, Jun. 2010.
- [2] B. Ottersten, M. Viberg and T. Kailath, "Analysis of subspace fitting and ML techniques for parameter estimation from sensor array data," *IEEE Trans. Signal Process.*, vol. 40, pp. 590-600, Mar. 1992.
- [3] P. Stoica and R. L. Moses, *Spectral Analysis of Signals*. Upper Saddle River, NJ, USA: Prentice-Hall, 2005.
- [4] R. Schmidt, "Multiple emitter location and signal parameter estimation," *IEEE Trans. Antennas Propag.*, vol. 34, no. 3, pp. 276-280, 1986.
- [5] R. Roy and T. Kailath, "ESPRIT-estimation of signal parameters via rotational invariance techniques," *IEEE Trans. Acoust., Speech, Signal Process.*, vol. 37, no. 7, pp. 984-995, 1989.
- [6] Z. Yang, J. Li, P. Stoica and L. Xie, "Sparse methods for direction-of-arrival Estimation," arXiv:1609.09596.
- [7] D. Malioutov, M. Cetin and A. Willsky, "A sparse signal reconstruction perspective for source localization with sensor arrays," *IEEE Trans. Signal Process.*, vol. 53, no. 8, pp. 3010-2022, 2005.

- [8] Y. Chi, L. L. Scharf, A. Pezeshki and R. Calderbank, “Sensitivity of basis mismatch to compressed sensing,” *IEEE Trans. on Signal Process.*, vol. 59, pp. 2182 - 2195, 2011.
- [9] B. Mamandipoor, D. Ramasamy and U. Madhow, “Newtonized orthogonal matching pursuit: Frequency estimation over the continuum,” *IEEE Trans. Signal Process.*, vol. 64, no. 19, pp. 5066-5081, 2016.
- [10] J. Fang, F. Wang, Y. Shen, H. Li and R. S. Blum, “Superresolution compressed sensing for line spectral estimation: an iterative reweighted approach,” *IEEE Trans. Signal Process.*, vol. 64, no. 18, pp. 4649-4662, 2016.
- [11] T. L. Hansen, B. H. Fleury and B. D. Rao, “Superfast line spectral estimation,” *IEEE Trans. Signal Process.*, vol. 66, no. 10, pp. 2511-2526, 2018.
- [12] L. Hu, J. Zhou, Z. Shi and Q. Fu, “A fast and accurate reconstruction algorithm for compressed sensing of complex sinusoids,” *IEEE Trans. Signal Process.*, vol. 61, no. 22, pp. 5744-5754, 2013.
- [13] L. Hu, Z. Shi, J. Zhou and Q. Fu, “Compressed sensing of complex sinusoids: An approach based on dictionary refinement,” *IEEE Trans. Signal Process.*, vol. 60, no. 7, pp. 3809-3822, 2012.
- [14] G. Tang, B. Bhaskar, P. Shah and B. Recht, “Compressed sensing off the grid,” *IEEE Trans. Inf. Theory*, vol. 59, no. 11, pp. 7465-7490, 2013.
- [15] Z. Yang and L. Xie, “On gridless sparse methods for line spectral estimation from complete and incomplete data,” *IEEE Trans. Signal Process.*, vol. 63, no. 12, pp. 3139-3153, 2015.
- [16] Y. Li and Y. Chi, “Off-the-grid line spectrum denoising and estimation with multiple measurement vectors,” *IEEE Trans. Signal Process.*, vol. 64, no. 5, pp. 1257-1269, 2016.
- [17] Z. Yang, L. Xie and C. Zhang, “A discretization-free sparse and parametric approach for linear array signal processing,” *IEEE Trans. Signal Process.*, vol. 62, no. 19, pp. 4959-4973, 2014.
- [18] S. Boyd and L. Vandenberghe, *Convex Optimization*, Cambridge University Press, 2004.
- [19] M. A. Badiu, T. L. Hansen and B. H. Fleury, “Variational Bayesian inference of line spectrum estimation,” *IEEE Trans. Signal Process.*, vol. 65, no. 9, pp. 2247-2261, 2017.
- [20] J. Zhu, Q. Zhang, P. Gerstoft, M. A. Badiu and Z. Xu, “Variational Bayesian line spectral estimation with multiple measurement vectors,” arXiv:1803.06497.
- [21] S. Rangan, T. S. Rappaport and E. Erkip, “Millimeter-wave cellular wireless networks: potentials and challenges,” *Proc. IEEE*, vol. 102, no. 3, pp. 366-385, 2014.
- [22] O. Mehanna and N. Sidiropoulos, “Frugal sensing: Wideband power spectrum sensing from few bits,” *IEEE Trans. on Signal Process.*, vol. 61, no. 10, pp. 2693-2703, May 2013.
- [23] Y. Chi and H. Fu, “Subspace learning from bits,” *IEEE Trans. on Signal Process.*, vol. 65, no. 17, pp. 4429-4442, Sept 2017.

- [24] F. Li, J. Fang, H. Li and L. Huang, "Robust one-bit Bayesian compressed sensing with sign-flip errors," *IEEE Signal Process. Lett.*, vol. 22, no. 07, 2015.
- [25] J. Fang, Y. Shen, L. Yang and H. Li, "Adaptive one-bit quantization for compressed sensing," *Signal Processing*, vol. 125, pp. 145-155, 2016.
- [26] G. Franceschetti, V. Pascazio, G. Schirinzi, "Processing of signum coded SAR signal: theory and experiments," *IEE Proceedings F - Radar and Signal Processing*, vol. 138, no. 3, pp. 192-198, Jun. 1991.
- [27] C. Gianelli, L. Xu, J. Li, P. Stoica, "one-bit compressive sampling with time-varying thresholds for sparse parameter estimation," *IEEE Sensor Array and Multichannel Signal Processing Workshop (SAM)*, Rio de Janeiro, Brazil, July 10-13, 2016.
- [28] J. Li, M. M. Naghsh, S. J. Zahabi, M. M. Hashemi, "compressive radar sensing via one-bit sampling with time-varying thresholds," *50th Asilomar Conference on Signals, Systems and Computers*, Pacific Grove, CA, USA, 6-9 Nov. 2016.
- [29] K. Yu, Y. Zhang, M. Bao, Y. Hu and Z. Wang, "DOA estimation from one-bit compressed array data via joint sparse representation," *IEEE Signal Process. Lett.*, vol. 23, no. 9, pp. 1279-1283, 2016.
- [30] X. Meng, J. Zhu, "A generalized sparse Bayesian learning algorithm for one-bit DOA estimation," *IEEE Commun. Lett.*, vol. 22, no. 7, pp. 1414-1417, 2018.
- [31] Y. Gao, D. Hu, Y. Chen, Y. Ma, "Gridless 1-b DOA estimation exploiting SVM approach," *IEEE Commun. Lett.*, vol. 21, no. 10, pp. 2210-2213, 2017.
- [32] C. Gianelli, L. Xu, J. Li, P. Stoica, "One-bit compressive sampling with time-varying thresholds for multiple sinusoids," *IEEE 7th International Workshop on Computational Advances in Multi-Sensor Adaptive Processing (CAMSAP)*, 10-13 Dec. 2017, Curacao, Netherlands Antilles.
- [33] C. Li, R. Zhang, J. Li and P. Stocia, "Bayesian information criterion for signed measurements with application to sinusoidal signals," *IEEE Signal Process. Lett.*, vol. 25, no. 8, pp. 1251-1255, 2018.
- [34] C. Zhou, Z. Zhang, F. Liu, B. Li, "Gridless compressive sensing method for line spectral estimation from 1-bit measurements," *Digital Signal Processing*, vol. 60, pp. 152-162, 2017.
- [35] H. Fu and Y. Chi, "Quantized spectral compressed sensing: Cramér-Rao bounds and recovery algorithms," *IEEE Trans. on Signal Process.*, vol. 66, no. 12, pp. 3268-3279, 2018.
- [36] C. J. Wang, C. K. Wen, S. Jin, S. H. Tsai, "Gridless channel estimation for mixed one-bit antenna array systems," *IEEE Trans. on Wireless Commun.*, vol. 17, no. 12, pp. 8485-8501, 2018.
- [37] T. Minka, "A family of algorithms for approximate Bayesian inference," Ph.D. dissertation, Department of Electrical Engineering and Computer Science, Mass. Inst. Technol., Cambridge, MA, USA, 2001.

- [38] X. Meng, S. Wu and J. Zhu, “A unified Bayesian inference framework for generalized linear models,” *IEEE Signal Process. Lett.*, vol. 25, no. 3, pp. 398-402, 2018.
- [39] D. L. Donoho, A. Maleki, and A. Montanari, “Message passing algorithms for compressed sensing: I. Motivation and construction” in *Proc. Inf. Theory Workshop*, Cairo, Egypt, Jan. 2010, pp. 1-5.
- [40] X. Meng, S. Wu, L. Kuang, and J. Lu, “An expectation propagation perspective on approximate message passing,” *IEEE Signal Process. Lett.*, vol. 22, no. 8, pp. 1194-1197, Aug. 2015.
- [41] S. Wu, L. Kuang, Z. Ni, J. Lu, D. Huang, and Q. Guo, “Low-complexity iterative detection for large-scale multiuser MIMO-OFDM systems using approximate message passing,” *IEEE J. Sel. Topics Signal Process.*, vol. 8, no. 5, pp. 902-915, May 2014.
- [42] S. Rangan, “Generalized approximate message passing for estimation with random linear mixing,” in *Proc. IEEE Int. Symp. Inf. Theory*, Jul. 2011, pp. 2168-2172.
- [43] S. Rangan, P. Schniter, and A. Fletcher, “Vector approximate message passing,” arXiv preprint arXiv:1610.03082, 2016.
- [44] P. Schniter, S. Rangan, and A. K. Fletcher, “Vector approximate message passing for the generalized linear model,” in *Proc. 50th Asilomar Conf. Signals, Syst. Comput.*, Nov. 2016, pp. 1525-1529.
- [45] D. P. Wipf and B. D. Rao, “Sparse Bayesian learning for basis selection,” *IEEE Trans. Signal Process.*, vol. 52, no. 8, pp. 2153-2164, 2004.
- [46] K. V. Mardia and P. E. Jupp, *Directional Statistics*. New York, NY, USA: Wiley, 2000.
- [47] K. P. Murphy, *Machine Learning: a Probabilistic Perspective*. MIT Press, 2012.
- [48] Bertsekas, D. P. and Tsitsiklis : *Parallel and Distributed Computation: Numerical Methods*, Athenan Scientific: Massachusetts, 1997.